Long-Term Impact of Cover Crop and Reduced Disturbance Tillage on Soil Pore Size Distribution and Soil Water Storage

Samuel N. Araya[1], Jeffrey P. Mitchell[2], Jan W. Hopmans[3], and Teamrat A. Ghezzehei[4]

[1]Earth System Science, Stanford University, Stanford, CA, USA
[2]Department of Plant Sciences, University of California, Davis, CA, USA
[3]Department of Land, Air and Water Resources, University of California, Davis, CA, USA
[4]Life and Environmental Science, University of California, Merced, CA, USA

Correspondence to: Samuel N. Araya (araya@stanford.edu)

Abstract. We studied the long-term impact of contrasting tillage and cover cropping systems on soil structure and hydraulic properties using laboratory measurements and numerical simulations. Complete water retention and conductivity curves for the top (0 – 5 cm) and subsurface (20 – 25 cm) soils were characterized and contrasted. Dynamic water storage and retention were evaluated using numerical simulations in HYDRUS-2D software. Compared to standard-till (ST) and no cover crop (NO) systems, soils under no-till (NT) and cover cropping (CC) systems showed improved soil structure in terms of pore size distribution (PSD). Changes in hydraulic conductivity (K) under these systems led to increased infiltration rate and water retention. However, NT and CC plots had lower water content at field capacity (33 kPa suction) and lower plant available water (PAW) compared to ST and NO plots. Numerical simulations, however, showed that NT and CC plots have higher water storage (albeit marginal in magnitude) and water availability following irrigation. Because the numerical simulations considered retention and conductivity functions simultaneously and dynamically through time, they allow the capture of hydraulic properties that are arguably more relevant to crops. The study concludes that the long-term practices of NT and CC systems were beneficial in terms of changes to the PSD. NT and CC systems also made marginal improvements in soil water conductivity and storage, improving water retention at the plot scale.

List of Acronyms and Symbols

CC, Cover crop; HCF, Hydraulic conductivity function; NT, No-till; PAW, Plant available water content; PSD, Pore size distribution; ST, Standard-till; WRC, Water retention curve

K_s, Saturated hydraulic conductivity; θ_{FC}, Volumetric water content at field capacity; θ_{PWP}, Volumetric water content at permanent wilting point (-15 MPa suction); ρ_b, Bulk density; h, Negative water suction ($h = -\psi$); K, Hydraulic conductivity; θ, Volumetric water content; ψ, Matric potential.

1 Introduction

55 Improving soil health—the vitality of a soil in sustaining the socio-ecological functions of its enfolding land (Janzen et al., 2021)—is one of the main challenges of our time as we grapple with the demands of growing population and changing climate. The tools at our disposal to achieve this goal in agricultural lands are collectively known as conservation agriculture practices. Conservation agriculture is characterized by a combination of three linked principles: (1) reduced mechanical soil disturbance, (2) preservation of a permanent organic soil cover, and (3) diversification of crop species (Kassam et al., 2019; Li et al., 2018;

60 Mitchell et al., 2019). The adoption of conservation agriculture has been growing worldwide at an increasing rate since the 1960s. Between 2008 and 2015, the global area under conservation agriculture increased by 69% to 180 M ha (Blanco-Canqui and Ruis, 2018; Kassam et al., 2019). In California's highly productive Central Valley region, the cultivated area under conservation agriculture for tomato and corn production has increased from less than 5,000 ha in 2004 to over 140,000 ha in 2012 (Mitchell et al. (2016a).

65 Conservation agriculture promises two main categories of benefits to soil health and soil functions. First, conservation agriculture (specifically reduced tillage) eliminates the negative effects associated with standard (conventional) tillage (ST) such as the degradation of soil structure, increased erosion, loss of nutrients, reduction in soil organic matter, and reduction in soil microbial diversity (Lal et al., 2007; Zuber and Villamil, 2016). Second, conservation agriculture supports the development of healthy soils. Several studies have shown, for example, that reduced disturbance tillage systems sequester more carbon and

70 decrease greenhouse gas emission (Reicosky and Allmaras, 2003; Palm et al., 2014; Sanz-Cobena et al., 2017); improve soil physical properties such as soil bulk density and penetration resistance (Veenstra et al., 2006, 2007); increase microbial biomass, richness, and activity (Zuber and Villamil, 2016; Martens, 2004; Johnson and Hoyt, 1999); and reduce dust and air particle pollution (Baker et al., 2005; Madden et al., 2008; Reicosky and Allmaras, 2003). While some studies show that reduced disturbance tillage reduced yield (Pittelkow et al., 2015), others have found that the yield is unaffected (Naab et al.,

75 2017; Rasmussen, 1999; Alvarez and Steinbach, 2009) while reducing cost (Upadhyaya et al., 2001; Mitchell et al., 2009; González-Sánchez et al., 2016). Cover cropping—planting between cropping seasons to maintain soil coverage throughout the year and often to replenish soil N—provides many beneficial services including soil cover, residues, and biological diversity (Mitchell et al., 2019). Cover crops have been shown to reduce erosion (Reicosky and Forcella, 1998; Shelton et al., 2000)

Deleted: negative

Deleted: grew

Deleted: ,

Deleted: ,

Deleted: ,

Deleted: ,

Deleted: including

Deleted: and soil organic matter

Deleted: .

Deleted: For

Deleted: have been shown to

Deleted: increase soil fertility

Deleted: improve environmental quality

Deleted: without compromising yield

diseases, and pest pressure (Mitchell et al., 2017); while increasing soil fertility (Büchi et al., 2018; Abdalla et al., 2019), as well as microbial biomass, richness, and activity (Fernandez et al., 2016; Duchene et al., 2017).

Conservation agriculture is also credited with various beneficial changes to soil hydrology, including increases in macroporosity (Abdollahi et al., 2014; Burr-Hersey et al., 2017), water storage (Liu et al., 2019; Basche et al., 2016a; Duchene et al., 2017; Finney et al., 2017; Ashworth et al., 2017), and infiltration (Hudson, 1994; Johnson and Hoyt, 1999; Basche and DeLonge, 2017). Mitchell (2017) found cover crops increased infiltration by 2.8 times compared to soils without cover crops. Based on a meta-analysis from 27 studies, Basche and DeLonge (2017) concluded that cover cropping was effective in enhancing soil water storage and other soil hydrologic properties when practiced for longer-term (> 10 years) and in drier environments (< 900 mm annual rainfall).

However, conservation agriculture can also lead to undesired negative outcomes. Without tillage to loosen the soil, reduced tillage systems can cause soil consolidation and compaction that can reverse the beneficial physical soil health outcomes (Blanco-Canqui and Ruis, 2018; Pittelkow et al., 2015). Several studies have noted the critical lack of field studies and the need for evaluation of long-term effects of conservation agriculture on the soil physical and hydraulic properties and soil hydrological processes (Peña-Sancho et al., 2016; Basche and DeLonge, 2017; Blanco-Canqui and Ruis, 2018; Bacq-Labreuil et al., 2019). In this study, we planned to assess the long-term individual impact and its interaction of reduced tillage and cover crops practices on soil structure and associated hydrologic soil functions. We evaluated the properties of soil cores collected from the California Conservation Agricultural Systems Innovation (CASI) Center, where plots have been under a mix of reduced tillage and cover crop treatments since 1999. Specifically, we aimed to test whether conservation agriculture results in significant alterations in water retention, pore size distribution, density, hydraulic conductivity as well as static and dynamic field capacity.

2 Methods

2.1 Study site and experimental design

The CASI study site is located at the University of California West Side Research and Extension Center in Five Points, California (36.34066°N, 120.1207°W, Figure 1). The experimental field has two-factor replicated treatments of tillage and winter cover cropping: standard-till with and without cover crops (ST-NO and ST-CC, respectively); and conservation tillage (no-till) with and without cover crops (NT-NO and NT-CC, respectively). CASI defines conservation tillage as a range of production practices that reduce primary intercrop tillage operations and either preserve 30% or more residue cover or reduce

Deleted: myriad

Deleted: 0

Deleted: For example,

Deleted: individual and interactive impacts

Deleted: Figure 1

Deleted: reduced disturbance
Deleted: tillage

the total number of tillage passes by 40% or more (Mitchell, 2016). Throughout this manuscript, we will use the more descriptive no-till (NT) instead of conservation tillage.

Each treatment combination was replicated eight times in a randomized complete block implemented on a 9 by 82-m dimension plot with an approximately 10-m buffer guard between the tillage treatments. All tractor and implement traffic were restricted to the furrows and planting beds were never moved. While the operations used varied from year to year, the number of tractor passes for the NT plots was always reduced by 40% or more relative to the ST plots (Mitchell et al., 2012). Both the ST and the NT systems were previously described in detail (Veenstra et al., 2006; Mitchell et al., 2016b). The NT systems were managed from the principle of reducing primary intercrop tillage to the greatest extent possible. Controlled traffic farming practices that restrict tractor traffic to certain furrows were used, and planting beds were not moved or destroyed in these systems during the entire study period. The only soil disturbance operations used in the NT systems were shallow cultivation during the first eight years of the project, since 2012. However, the only soil disturbance occurs at the time of seeding or transplanting. The ST systems consisted of multiple conventional intercrop tillage operations which break down and establish new beds following harvest and represent the normal operations of the San Juaquin Valley in terms of intensity, depth, and timing of tillage.

The soil type at the study site is a Panoche clay loam (fine-loamy, mixed, superactive, thermic Typic Haplocambids) which is representative of much of California's Central Valley. The particle size distribution of the soil is 25% sand, 37% silt, and 39% clay. Based on 2012-2014 measurements, the organic carbon content of the top 15 cm soils is 13.9 g cm^{-3} for ST-NO, 16.95 g cm^{-3} for ST-CC, 21.56 g cm^{-3} for NT-NO, and 25.53 g cm^{-3} for NT-CC plots (Mitchell et al., 2017). For the first 12 years of the conservation agriculture experiment (between 2000 and 2012), tomato and cotton were grown in rotation, followed by a rotation of sorghum with garbanzo beans since 2012. All plots were irrigated by subsurface drip.

The cover crops were a mix of triticale (*Triticosecale Wittm*), cereal rye (*Secale cereale L.*), common vetch (*Vicia sativa*), radish (*Raphanus sativus*), and clover (*Trifolium incarnatum*) seeded in 20 cm rows at 89.2 kg ha- in late October. The cover crops are terminated in late March of the following year using a stalk chopper followed by disk incorporation in the ST system or sprayed with a 2% solution application of glyphosate after chopping and left on the surface as a mulch in the NT systems. Detailed descriptions of the study site and management have been published in previous works (Mitchell et al., 2017, 2015; Veenstra et al., 2006; Mitchell et al., 2016c)

Figure 1 Study site location at Five Points, California (California's Central Valley extent map from Faunt (2012)).

155 **2.2 Sampling**

Sampling was done in mid-November 2017, aproximately 5 months after tillage in the ST treatment plots to avoid the immediate effects of tillage since we were primarily interested in the long-term effects of the treatments. Tillage operations have a transitory effect on porosity and associated soil hydraulic properties as structures collapse, mainly driven by wetting and drying cycles post tillage (Or et al., 2000; Mapa et al., 1986). The immediate alterations of tillage on soil porosity and

160 hydraulic properties have been shown to diminish rapidly following only a few wetting and drying cycles (Strudley et al., 2008; Alletto et al., 2015; Green et al., 2003).

Undisturbed soil samples from the top (0 – 5 cm) and subsurface (20 – 25 cm) layers were collected carefully using a 250 cm^3 volume sampling ring (8 cm diameter by 5 cm height). The depths were chosen to correspond with the depth disturbed by disking to incorporate residue in the ST plots (i.e., 0 – 20 cm depth) (Mitchell et al., 2015; Veenstra et al., 2006) and the deeper

165 layer. Samples were collected along the strip ridges within the plots away from the trafficked furrows but slightly off-center to avoid drip irrigation tubes that were buried at the center of ridges. A total of 32 samples were collected by taking one surface and one subsurface sample from four of the eight treatment replicate plots. This resulted in four replicates of surface and subsurface samples per treatment. The samples were stored at 4 °C before laboratory analysis.

Deleted: ,

 2.3 Laboratory measurements

To assess the long-term impact of NT and CC practices on soil structure, we measured soil bulk densities (ρ_b), total porosities, pore size distributions (PSD), and soil hydraulic properties of water retention (WRC) and hydraulic conductivity functions (HCF).

The saturated hydraulic conductivity (K_s) was measured using the falling-head method. For this method, soils were saturated by immersing sample cores in degassed, 0.01 M $CaCl_2$ solution so that the water level was close to the rim. K_s of the saturated soil was then measured by the falling-head method using the KSAT instrument (METER Group, Inc., Munich, Germany) by allowing a 5 cm column of degassed, 0.01 M $CaCl_2$ solution to flow through the soil core. The setup was such so that the flow direction was downward. Following the K_s measurement, soil WRC, and HCF data were determined simultaneously using the evaporation method as developed for the HYPROP instrument (METER Group, Inc., Munich, Germany). The HYPROP simultaneously measures, at high frequency (10 min), suction inside the soil cores at two different depths along with weight loss while saturated soil cores dry. This allows for the calculation of WRC, $\theta(\psi)$, and HCF, $K(\psi)$. Following the HYPROP measurements, soil water retention in the range of water tensions from 10^3 to 10^6 cm was determined by using the WP4C instrument (Decagon Devices, Inc, Pullman, WA, USA).

We define field capacity (θ_{FC}) and permanent wilting point (θ_{PWP}) as the volumetric water content with the corresponding volume of water retained in the soil at 33 kPa and 1,500 kPa suction, respectively. θ_{FC} and θ_{PWP} are approximations of water retained after internal drainage has ceased, and the soil water content limit at which plants cannot recover from turgidity, respectively (Hillel, 1998). We calculated plant available water (PAW) as the difference between θ_{FC} and θ_{PWP} (i.e., $PAW = \theta_{FC} - \theta_{PWP}$). In addition to the saturated hydraulic conductivity, we also compared the unsaturated hydraulic conductivity near field capacity water content at -10 kPa. A near-saturated hydraulic conductivity, such as at -10 kPa, may better represent infiltration in the field since 100% saturation is unlikely under field conditions due to factors such as air entrapment.

Throughout this manuscript, the term water suction, h, is used to represent the soil water matric potential, ψ, such that $h = -\psi$ (cm).

2.4 Soil porosity determination

Total soil porosity (P) was calculated as $P = 1 - \rho_b/\rho_p$, where ρ_p is the particle density of soil, taken as 2650 kg m^{-3}, and ρ_b is the soil bulk density determined using the standard core method (Grossman and Reinsch, 2002).

Deleted: measure
Deleted: the
Deleted: y
Deleted: y
Deleted: (
Deleted: curve,
Deleted: ,
Deleted: ,
Deleted: of the soil cores

Deleted: use the conventional definition
Deleted: for
Deleted: −
Deleted: −
Deleted: ,
Deleted: calculated

The effective pore size distribution (PSD) was estimated from the slope of the WRC using the differential water capacity (Klute, 1986). For this, the WRC—$\theta(h)$—was first transformed into a curve of effective saturation (S) as a function of effective pore radius (r), $S(r)$. S was calculated as $S = (\theta - \theta_r)/(\theta_s - \theta_r)$, where θ_s and θ_r are the saturated and residual volumetric water contents estimated from a bimodal constrained van Genuchten model fit (Durner, 1994) of measured WRC. The draining pore radius was approximated using the Young-Laplace equation (1):

$$r = \frac{2\gamma \cos(\beta)}{\rho_w g h} = \frac{1490}{h} \tag{1}$$

where r [µm] is pore radius, h [cm] is the suction, γ is the surface tension between water and air (0.0729 N m^{-1}), β is the contact angle (assumed 0), ρ_w is the density of water (1000 kg m^{-3}), and g is the acceleration due to gravity (9.81 m s^{-2}). The PSD curves were then calculated as (2):

$$f_p(\ln r) = -\frac{dS}{d \ln r} \tag{2}$$

where f_p [-] is the density function of effective pore sizes. Prior to calculating PSD, the $S(r)$ curve was fitted with a cubic smoothing spline to remove noise in the measurement data (Kastanek and Nielsen, 2001; Pires et al., 2008). For a deeper insight, we divided pore sizes into four ranges: intra-microaggregates (<0.2 µm), intra-aggregates (0.2 – 10 µm), small macropores (10 – 50 µm), and large macropores (50 – 1000 µm). These range categories allowed us to perform statistical comparisons on the relative abundance of the pore size ranges among the different treatments.

2.5 Soil water storage simulations

To measure the interactive impact of changes in WRC and HCF on profile water dynamics and storage, we conducted a numerical simulation of field irrigation. The fate of irrigation water applied on the different treatment plots was simulated in HYDRUS-2D software, where water flow is modeled using a modified form of the Richards' equation (Equation 3) which incorporates a sink term to account for water uptake by plant roots (Simunek et al., 2012).

$$\frac{\partial \theta}{\partial t} = \frac{\partial}{\partial x_i}\left[K\left(K_{ij}^A \frac{\partial h}{\partial x_j} \right) \right] - S_r \tag{3}$$

where θ [L^{3}L^{-3}] is the volumetric water content, t [T] is time, x_i [L] are the spatial coordinates, K [LT^{-1}] is the unsaturated hydraulic conductivity, K_{ij}^A [-] are the components of a dimensionless anisotropy tensor, h [L] is the pressure head, and S_r [T^{-1}] is the sink term representing the rate of water volume removed due to plant water uptake.

The domain was set up as an axisymmetric cylinder of 18 cm radius and 100 cm depth. Figure 2 illustrates the model domain sketch and the domain setup in HYDRUS-2D. The domain was discretized with 1473 nodes and 2788 triangular elements. This discretization mesh was refined to have more nodes around the emitter (0.5 cm spacing) and soil layer boundaries (1 cm spacing) to capture expected high rates of changes in soil moisture. The material distribution in terms of soil hydraulic properties was such that the top 0 – 20 cm and the subsurface 20 – 30 cm were those measured in this study (Section 3.3). Soil hydraulic properties for the bottom layers, 30 – 60 and 60 -100 cm layers, were predicted from soil characteristics using Rosetta-H5 pedotransfer function (Schaap et al., 2001) and the van Genuchten-Mualem hydraulic model (van Genuchten, 1980). Soil characteristics for these layers were based on soil properties of C1 and C2 soil horizons (41 – 58 and 58 – 91 cm depths, respectively) for Panoche soils, Pedon ID S1978CA029001 (National Cooperative Soil Survey, n.d.).

Subsurface irrigation emitter was represented with a sphere of 1 cm radius buried 10 cm below the surface. We simulated the fate of 4.8 cm depth equivalent irrigation applied at an emitter discharge rate of 0.61 l h^{-1} (0.60 cm h^{-1} equivalent irrigation depth) in each of the 16 sampled plots.

The entire domain surface area (1017.9 cm^2) was associated with transpiration and the root water uptake (S_r in in equation 3) was modeled by the HYDRUS-2D default Feddes' parameters for a tomato plant. The plant root water uptake spatial distribution model was implemented using Vrugt et al. (2001) functions with parameters given in Table 1.

Table 1 Feddes root model parameters and values.

Variable	Value (cm)
Maximum rooting depth	35
Maximum rooting radius	15
Depth of maximum uptake intensity	10
Radius of maximum uptake intensity	0 (at center)

An atmospheric boundary condition was set for the surface layer and a free drainage lower boundary for the bottom layer. The atmospheric boundary condition was defined by potential crop evapotranspiration (ET_c) which was calculated based on equation 4.

265

$$ET_c = K_c \times ET_0 \tag{4}$$

Where ET_c [LT^{-1}]is potential crop evapotranspiration, K_c [-] is crop coefficient (= 1.15 for tomato mid-season (Allen et al., 1998), and ET_0 [LT^{-1}] is the reference potential evapotranspiration.

Hourly reference potential evapotranspiration (ET_0) for a week (May 6 to 12, 2018) were retrived from the nearest weather station (CIMIS Five Points Station, https://cimis.water.ca.gov/).

270
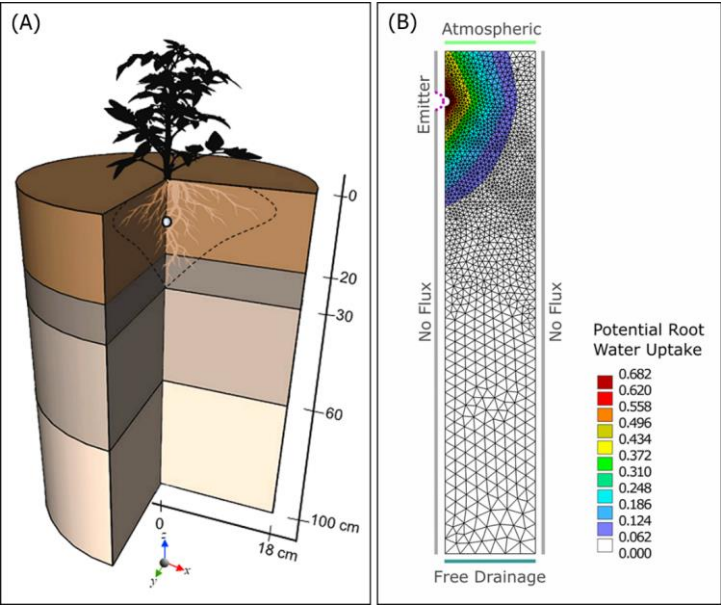
Figure 2 (A) 3D schematic representation of the domain geometry and material distribution. (B) Domain setup in Hydrus-2D showing the finite element mesh, related boundary conditions, and potential root water uptake rate distribution.

The starting pressure head of the entire model domain was set to -1000 cm, and simulation was initialized by a 14-week spin-

275 up period. The model was run recursively with 2.5 cm equivalent depth irrigation applied at the start of every week for 14

weeks after which the final simulation is run with 4.8 cm equivalent depth irrigation (at the rate of 0.6 cm h^{-1} for 8 h) application (Figure 3). The amount of water retained in a given soil profile layer following irrigation is calculated as equivalent water depth changes using Equation 5.

$$\Delta W_t = W_t - W_{t0} \tag{5}$$

where ΔW_t [L] is equivalent water depth retained in the soil profile t hours after irrigation application, W_t is the equivalent water depth in the soil profile t hours after irrigation, and Wt_0 is equivalent water depth immediately before irrigation application.
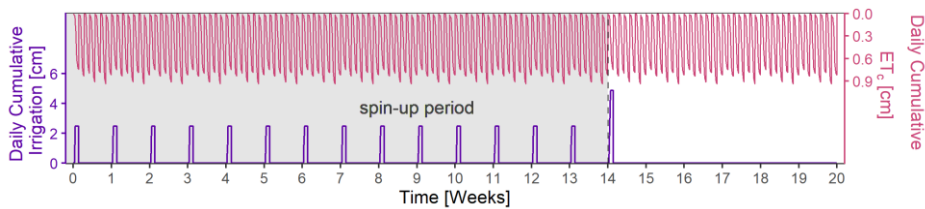
Figure 3 Daily cumulative irrigation and potential crop evapotranspiration through the 14 weeks of spin-up period (grey background) and the final simulation.

2.6 Statistical analysis

All quantitative results are expressed as means of four replicates ± standard error unless otherwise indicated. Differences in means were tested by analysis of variance (ANOVA) and pairwise comparison of treatments done using Tukey's honest significant difference (HSD) test at $p < 0.15$ significance level unless otherwise stated (Least Significant Difference table are provided in Appendix A Table B1). Hydraulic conductivity values were log-transformed before statistical analysis to make their distribution more normal. The normality of the data and the homogeneity of variances were checked using Shapiro–Wilk's and Levene's tests, respectively. All statistical analyses were performed using R statistical software (R Core Team, 2019).

3 Results and Discussion

An example of water conductivity and retention measurement for a single soil sample is shown in Figure 4. The HCF and WRC for all the samples are provided in Appendix A, Figures A1 and A2.
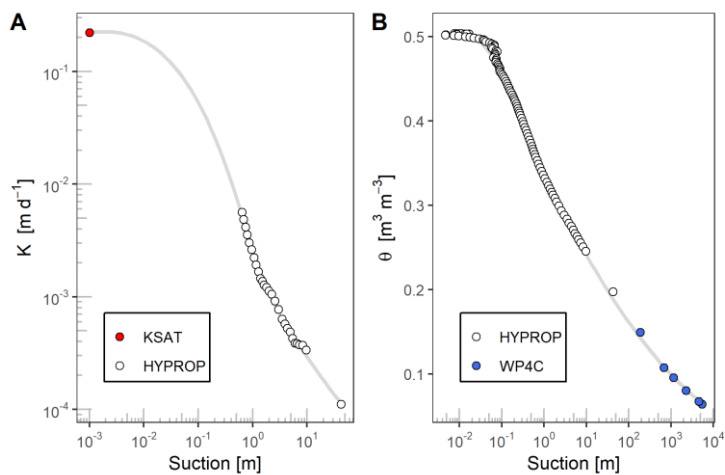
Figure 4 Plot of measured hydraulic conductivity (A) and water retention (B) for one of the topsoil ST-CC samples with the measurement instrument labeled. Grey lines are LOESS smooth trend lines.

3.1 Pore size distribution

The mean soil PSDs for the different systems are shown in Figure 5 (A). PSD curves for the individual samples are provided in Figure A3. A wider spread of PSD implies a heterogeneous mix of pore sizes and is indicative of soil with a more developed structure. The maximum pore volume density for the top soils occurred between sizes 15 and 20 µm diameter pores with the exception for NT-CC soils which showed a bimodal distribution with maximum pore volume density around 4 and 518 µm (Table 2).
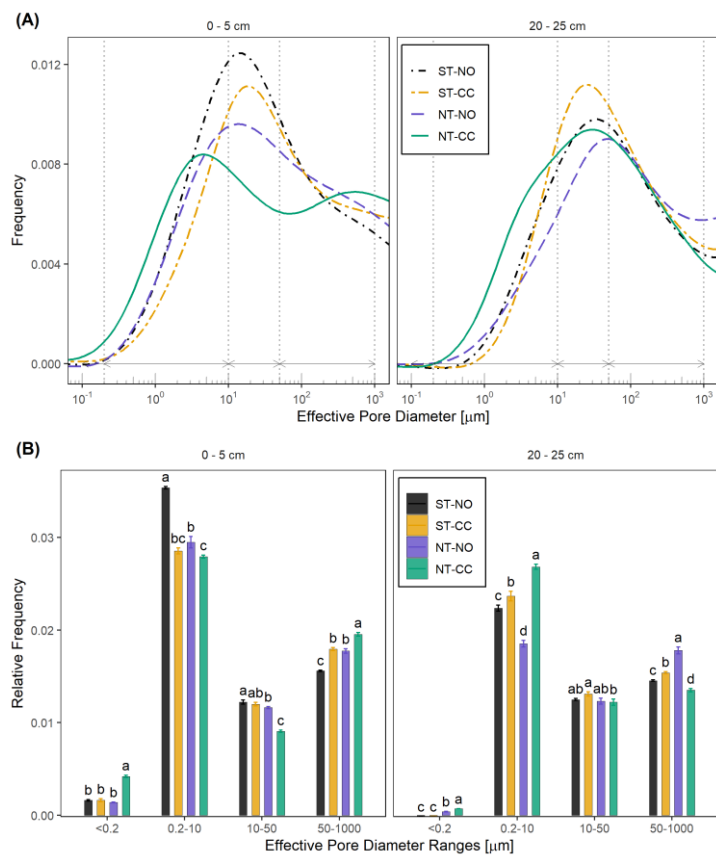
Figure 5 (A) Pore size distribution for the top (0 – 5 cm) and subsurface (20 – 25 cm) soil layers. Dotted vertical lines and horizontal arrows indicate the characteristic pore diameter ranges of <0.2, 0.2 – 10, 10 – 50, and 50 – 1000 μm. **(B)** The relative abundance of the four characteristic pore diameter ranges. Bars indicate standard errors. Different letters within the same pore size range indicate differences at p < 0.15.

325

Deleted: statistically significant

One observation is that the topsoil NT-CC has the widest spread of PSD, with statistically more proportion of the smaller and larger diameter pores (i.e., <0.2 µm and 50 – 1000 µm, respectively, at p < 0.15) and a bimodal distribution which is not present in the other systems (Figure 5B). Several studies have similarly observed an increase in the proportion of larger pores in NT systems (Tavares Filho and Tessier, 2009; Pires et al., 2017; Gao et al., 2019, 2017). The reason for the abundance of small and large pores for the NT-CC systems suggests the formation of tightly packed aggregates with smaller pores and larger interaggregate pores between them. This would be consistent with results from a previous study of our site and others that found higher aggregate stability for the NT-CC systems (Mitchell et al., 2017; Gao et al., 2019). Greenland (1977) suggests soil pore size classification based on equivalent diameter into three groups as transmission (50 – 500 µm), storage (0.5 – 50 µm), and residual pores (< 0.5 µm). Larger transmission pores are important for infiltration, drainage, and aeration while smaller storage pores are important in retaining water. Increased aeration of soil is beneficial for many soil processes including soil organic matter cycling (Lehmann and Kleber, 2015; Janzen, 2015) and other biogeochemical processes (Ekschmitt et al., 2008; Schmidt et al., 2011). ST-NO plots had the lowest relative abundance of larger macropores (50 – 1000 µm) while NT-CC had the highest proportion (Figure 5B).

Table 2 Modal diameter [µm] of the pore size distribution curves.

Depth	ST-NO	ST-CC	NT-NO	NT-CC
0 - 5 cm	14	19	14	4 and 518
20 - 25 cm	33	25	47	30

For the subsurface soils, the combined effect of NT and CC increased the spread of PSD however, NT without CC showed a narrower PSD with the highest PSD mode and highest abundance of large macropores compared to other treatments. NT-CC plots showed a higher proportion of intra-aggregate size pores and smaller (< 10 µm) at p < 0.15. Plant roots are important actors in soil structure development, they enhance aggregation by compacting soils through growth and exudation of segmenting materials, and also fragmenting aggregates to create larger interaggregate pores (Jarvis, 2007; Angers and Caron, 1998; Meurer et al., 2020). Given the reduced tillage in the NT plots, it could be that CC play a more critical role in forming more diverse aggregate sizes and wider PSD. The effect of the CC species should also be considered in this interpretation since it has recently been shown that the effect of CC on soil structure and porosity varies significantly with root morphology and architecture of the CC plant (Bacq-Labreuil et al., 2019).

3.2 Bulk density

There was a marked differences in ρ_b between the top and the subsurface layers regardless of the treatment type. The average ρ_b for the top and subsurface layer soils were 1.19 and 1.46 g cm^{-3}, respectively (which is equivalent to total porosities of 55 and 45 percent). Between the treatments, there was no statistically significant difference in ρ_b of subsurface soils at $p < 0.15$. For topsoils, only NT-NO soils showed a markedly higher ρ_b particularly compared to ST-NO (p = 0.078) and NT-CC (p = 0.141) (Figure 6). This observation tends to support one of the concerns of NT practice which is that NT practices may lead to soil consolidation and an increase in compaction because of the lack of intensive tillage (Blanco-Canqui and Ruis, 2018; Moret and Arrúe, 2007). Compaction reduces soil pore volume and affects soil fertility by reducing water flow and aeration, which negatively affect soil biological activity and redox potential (Vereecken et al., 2016). Our findings show that continued long-term NT led to a slight increase in compaction, however this effect was not found when NT was practiced with CC. The PSD we observed in NT systems (discussed in section 3.2), however, apear to imply that NT systems led to PSD indicative of a better-developed soil structure with primary and secondary structures.
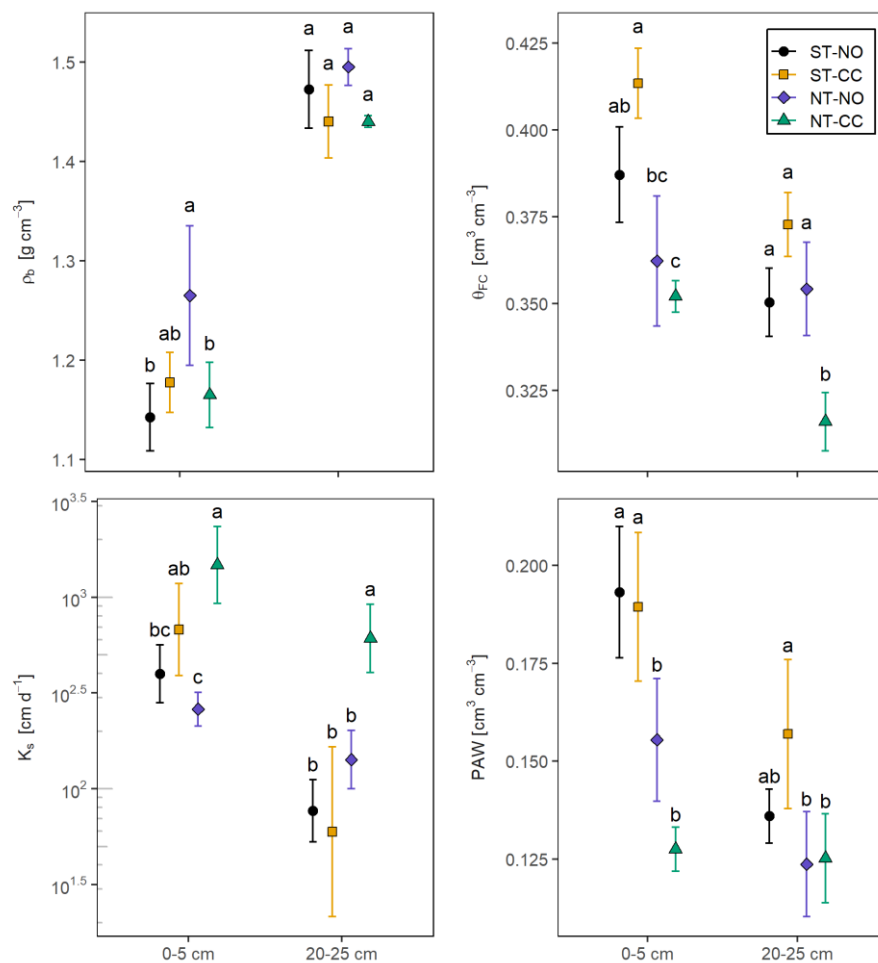
Figure 6 Mean bulk density (ρ_b), saturated hydraulic conductivity (K_s), water content at field capacity (θ_{FC}), and plant available water (PAW) of the top ($0 - 5$ cm) and subsurface ($20 - 25$ cm) layer soils. Bars indicate standard errors. Different letters within the same depth indicate differences at p < 0.15.

3.3 Hydraulic conductivity

The CC treatments tended to have a greater impact on K_s than the tillage treatment for the top layer soils (Figure 6). This is consistent with the increased in infiltration for these CC plots reported by Mitchell et al. (2017) where they noted a 2.8 times higher infiltration compared to the plots withoug CC. Mitchell et al. (2017) suggest several possible explanations including increased slaking associated with ST, better formation of macropores, and better continuity of soil pores possibly due to better-established soil structure and biology (Pires et al., 2017; Schwen et al., 2011). Both the top andd subsoil layer under NT-CC systems showed higher K_s compared to all the other treatments. These results suggest that CC is even more important in NT systems inorder to increase infiltration. We also compared conductivity at 100 cm suction, $K(100\ cm)$, as this may be a better representation of flow that is controlled by smaller pores as opposed to K_s. We found no aparent differences in $K(100\ cm)$ among the treatments.

3.4 Water retention

The NT treatments had lower θ_{FC} compared to ST (Figure 6). The larger value of θ_{FC} for ST plots are consistent with a more loose soil due to tillage increasing the capillary size pores. The θ_{FC} for the top layer NT soils were lower by more than 5 % volumetric water content (p<0.016) compared to ST-CC. The ST-NO treatments had intermediate values that were not statistically different (p<0.15) from all other treatments except NT-CC. The θ_{FC} showed similar trends for the subsurface layer soils but with smaller magnitudes of differences. CC appeared to enhance the effects of NT in terms of θ_{FC} and PAW of topsoil layers (Figure 6). The NT-NO top layer soils showed values between NT-CC and the ST soils. The top layers of NT-CC plots showed a marked decrease in PAW (p < 0.014) compared to the ST treatments. Assuming the top sample PAW represents 0 – 20 cm depth and the subsurface PAW represents 20 – 40 cm depths, the NT-CC soils would store 5.05 cm of equivalent surface water in plant-available form on the top 40 cm soil profile. This is 1.70 cm less plant available equivalent surface water per 40 cm depth compared to the average of the ST systems. The differences in PAW among the systems was mainly driven by θ_{FC} rather than θ_{PWP}. On both layers, the CC treatment increased θ_{FC} of ST soils but had the opposite effect on the NT soils. While some studies reported an increase in θ_{FC} and PAW with CC (Basche et al., 2016b; Bilek, 2007; Villamil et al., 2006), our findings are consistent with the observations from a recent meta-analysis of 93 paired observations of CC (Basche and DeLonge, 2017) which showed that CC did not affect total porosity for treatments practiced longer than 7 years or clay contents > 25 % which match the parameters of our study site. Our findings also agree with the findings of Basche and DeLonge (2017) in terms of θ_{FC}, they find that while long-term CC tends to increase θ_{FC}, it actually tends to decrease it for soils with >25% clay. Our results showed that while this was the case with ST, it was not the case for NT. For the subsurface layer of NT treatments, θ_{FC} was significantly lower for the NT-CC compared with NT-NO treatments. This difference suggests that roots

from cover crops extend below our surface layer and have the potential to significantly alter soil structure. This subsurface effect of CC may be masked by frequent disturbance in the ST treatments. This observation is consistent with recent studies that have shown that the effect of cover crops extends below the so-called plough layer (rooting depth of approximately 30 cm) (Rath et al., 2021; Veloso et al., 2018; Sastre et al., 2018; Tautges et al., 2019).

475 **3.5 Simulated water storage**

The simulation results showed that the difference in soil water content between the different treatments is most distinct in the top 40 cm. Figure 7 shows the vertical distribution of soil moisture following the irrigation for selected times. The 2-dimension distribution of soil moisture is shown in Appendix A Figures A4 and A5. Throughout the dry down following irrigation, the CC plots maintain higher volumetric water content in the top 20 cm. In the underlying 20 – 30 cm depth layers, however, the
480 NT-CC plots maintain the lowest soil moisture. While the NT-NO plots maintain a moderate soil water content in the top 20 cm compared to the other treatments, these plots maintain the highest water content in the 20 – 30 cm depth layers.
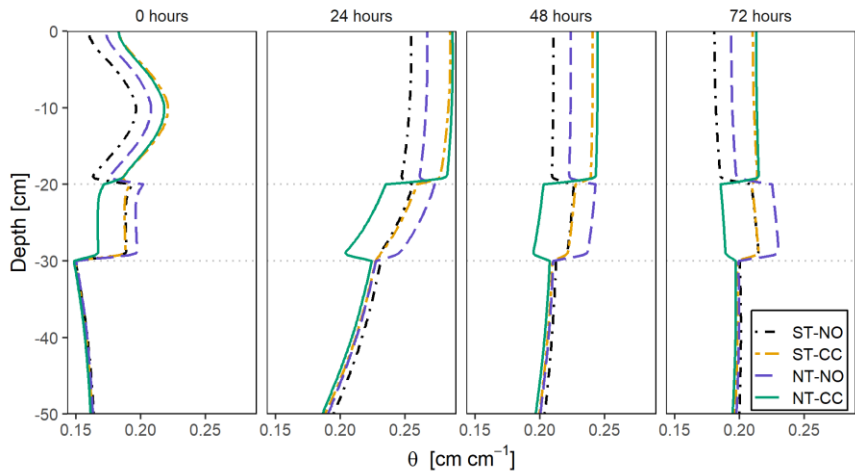
Figure 7. Vertical soil water content distribution 0-, 24-, 48- and 72-hours after irrigation (treatment means). Grey, dotted horizontal lines indicate the different soil boundaries.

485

Changes in water storage over time following 4.8 cm equivalent depth irrigation (see Equation 5) are shown in Figure 8. The results show that immediately following the end of irrigation, the top 40 cm layers start to lose water (to evapotranspiration

490   and drainage) while the deepest layer (60 – 100 cm) continues to gain water past 5 days after irrigation.
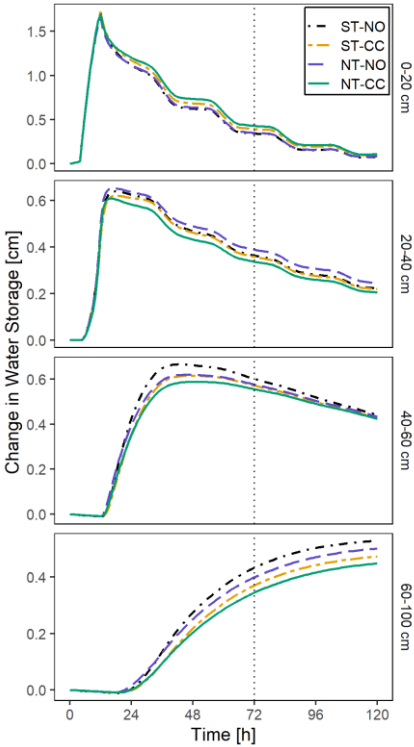
Figure 8. Change in water storage across soil layers (treatment means). Grey, dotted vertical line indicates day three after irrigation.

The conventional measure of plant-available water storage ($PAW = \theta_{FC} - \theta_{PWP}$) relies only on the WRC. Since WRC is a

495   description of soil water status at equilibrium, this measure of plant-available water does not account for the dynamic

interactions of water retention and hydraulic conductivity (Twarakavi et al., 2009). An alternative measure of field capacity is the "dynamic field capacity" which can be defined as the amount of water maintained in the soil after excess gravitational water is drained and the rate of downward movement is minimal (Veihmeyer and Hendrickson, 1931). This dynamic field capacity is commonly taken as the water content after three (or sometimes even five) days of drainage (Twarakavi et al., 2009; Assouline and Or, 2014). In our simulation, the rate of water drainage for the top and middle layers had significantly decreased after three days (Figure 8).

Comparison of the treatment averages in volumetric water content and amount of water retained three days after irrigation (that is the dynamic field capacity and water storage at time of field capacity) are shown in Figure 9. The magnitude of differences among all treatments were marginal (in the order of mm) but tended to favor the NT and CC treatments. In terms of change in water storage, the top 20 cm soils of the NT-CC plots retained the most water while the ST-NO plots retained the least amount of water. Water content at dynamic field capacity for the top 20 cm soils was marginally higher for CC plots compared to the NO plots with the ST-NO plots showing lowest water content (p < 0.09) than the CC plots. For the 20 – 40 cm depths, there was a contrast between NT-NO and NT-CC plots with NT-NO holding the most water and NT-CC holding the least amount. Among the 20 – 40 cm depths ST plots, there was no aparent difference in water content or water storage change three days after irrigation. These findings of water content at field capacity contrast with the θ_{FC} and PAW estimated from the conventional equilibrium measures (see Figure 6) which showed that the ST plots, in general, had higher water contents at field capacity and higher PAW. The dynamic water content at field capacity for the subsurface layers 20 – 30 cm shows similarity with that of the conventional field capacity for 20 -25 cm soils in that the NT-CC plots have lower water contents compared to NT-NO (p < 0.06). The ST plots 20 – 40 cm have water content at dynamic field capacity closer to that of NT-NO. Unlike the conventional equilibrium measures, the dynamic water storage and water contents at field capacity capture the interaction between water retention curve and hydraulic conductivity functions, therefore these measures likely capture soil hydrology more accurately.

Figure 9. Dynamic field capacity (θ_{FC}) and water storage change day three after irrigation. Bars indicate standard errors. Different letters indicate differences at p < 0.15.

560

4 Conclusion

Soils under long-term NT and CC practices showed a marked difference in soil pore size distribution (PSD). When practiced independetly, soils under NT and CC practices showed only moderate increase in PSD range and a very small or negligeable effect on the measured and simulated soil hydraulic properties. When practiced together, soils under NT-CC practices showed

565 the most pronounced changes in soil structure and hydraulic properties. Soils under NT-CC systems showed a bimodal PSD

in the top (0 –5 cm) soils with the modes around 4 and 500 µm effective diameter sizes, these modes are in the storage and transmission pore size categories. While ST is mainly done to loosen the top soil and improve soil structure for crops, its effect is transitory. Our results suggest that in the longer term, NT and CC practices increase soil aggregation and the proportion of larger pores while also maintaining total porosity.

CC practices, with or without tillage, tended to increase the saturated hydraulic conductivity (K_s) but appeared particularly effective when practiced in conjunction with NT. When practiced without CC, top layer soils (0 – 5 cm) under NT practices showed lower K_s even more than ST soils. The K_s of NT-CC subsurface layer (20 – 25 cm) tended to be higher than all other systems.

The measured water retention suggested a decrease in soils' ability to store water. The NT-CC practices decreased the calculated plant-available water (PAW) and water content at field capacity (θ_{FC}). While these equilibrium measures of field capacity and PAW indicate soil's ability to store water, the dynamically simulated water storage in soils is the result of the interaction between soil's water retention characteristics and its hydraulic conductivities. Both the water retention and conductivity are accounted for in the HYDRUS-2D irrigation simulation. The results showed that when both retention and conductivity properties are considered together, the top layers of NT systems not only do not show a disadvantage but have a marginally increased ability to store water compared to ST plots.

The changes in PSD associated with long-term NT and CC systems we observed suggest that these systems are beneficial to the improvement of soil structure. NT and CC systems also made marginal improvements in soil water conductivity and storage, improving water retention at the plot scale.

These soil measurements and simulation results reveal important changes that result from long-term conservation management. Future studies with more variety of soils and climate, as well as larger sample and replicate sizes, could to further illucidate the nuanced implications of the long-term effects of conservation agricuture.

Appendix A: Individual samples measurement curves and supplemental figures
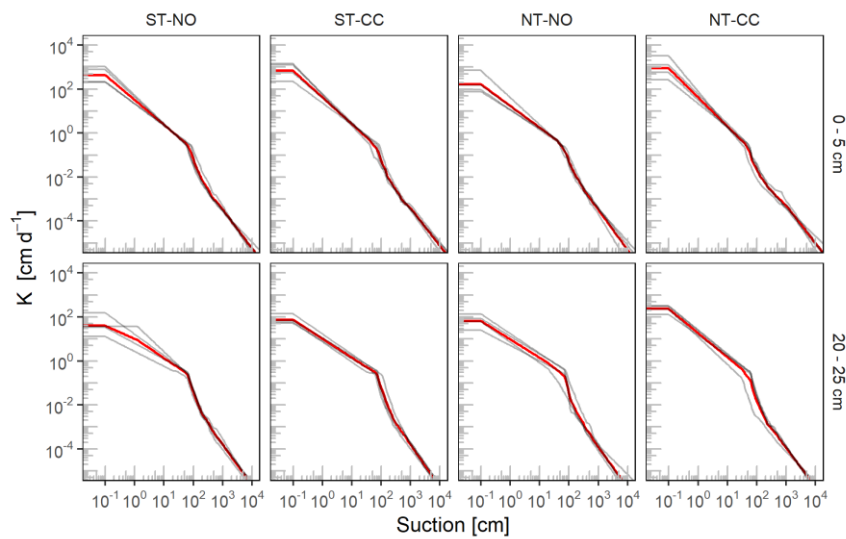
Figure A1 Hydraulic conductivity functions of top and subsurface layers by treatment. Grey curves are individual soil core measurements and thick red curves are the treatment means.

635
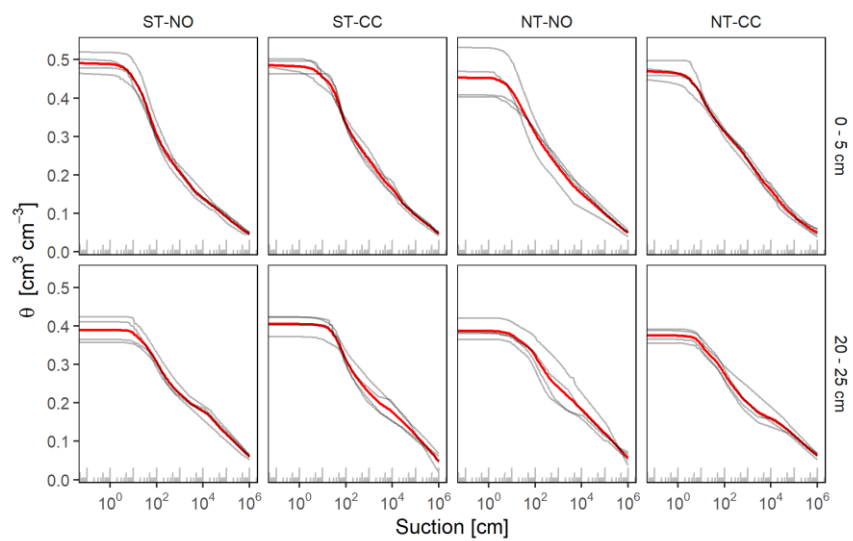
Figure A2 Water retention curves of top and subsurface layers by treatment. Grey curves are individual soil core measurements and thick red curves are the treatment means.

640
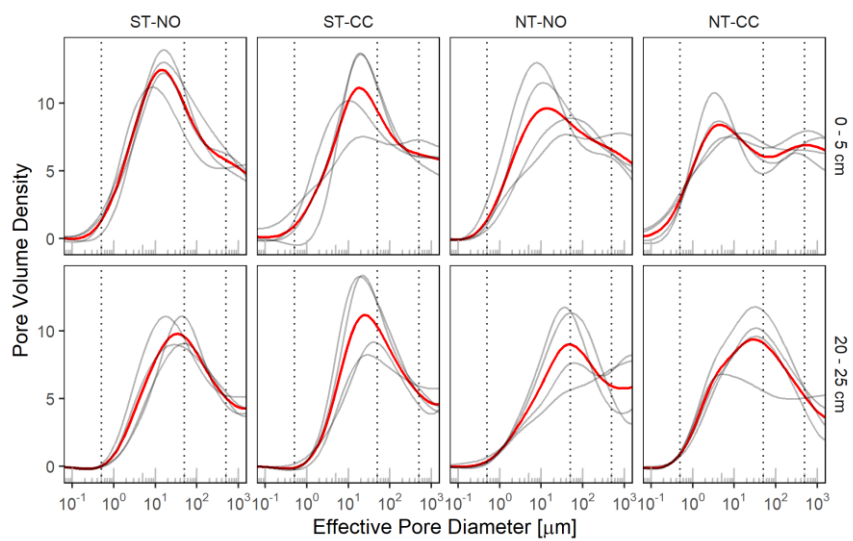
Figure A3 Effective pore size distribution. Grey curves are individual soil core measurements and thick red curves are the treatment means. Vertical dotted lines indicate pore diameter sizes of 0.5, 50, and 500 μm.

Deleted: means of the replicates
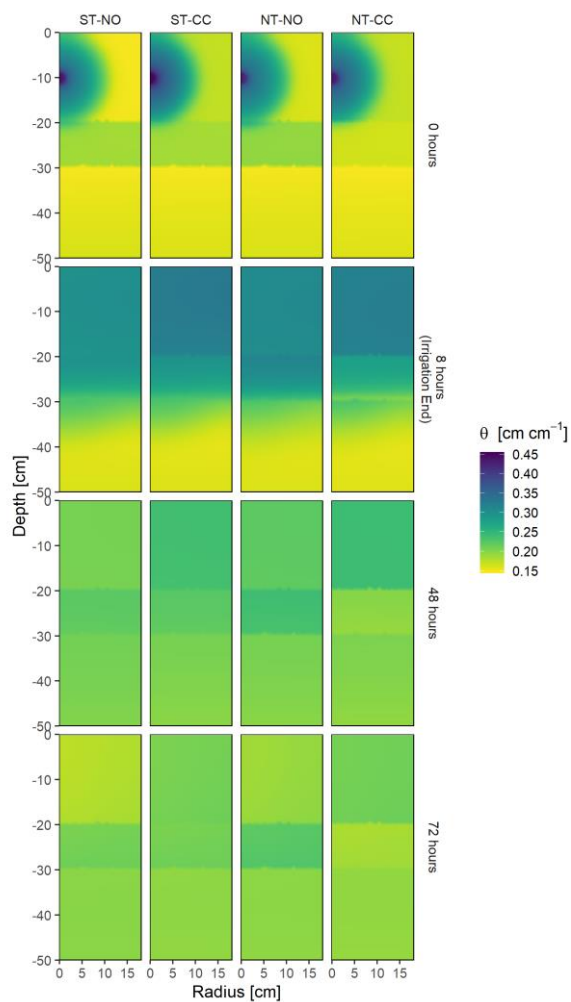
Figure A4 Soil water content distribution in the model domain at the start of irrigation and 0-, 48-, and 72-hours after irrigation (treatment means).

Figure A5 Hydraulic head distribution in the model domain at the start of irrigation and 0-, 48-, and 72-hours after irrigation (treatment means).

Deleted: Hydraulic

Appendix B: Statistical comparison of treatments

Table B1: Tukey's HSD test comparison of means for soil hydraulic properties. Tukey's HSD comparison of means. P-values < 0.15 are printed in bold and p-values < 0.05 bold and underlined. LCL and UCL are lower and upper control intervals, respectively.

Variable [unit]	Depth Range [cm]	Comparison	Difference	P-value	LCL	UCL
ρ_b [g cm^{-3}]	0-20	NT-CC -- NT-NO	-0.1	**0.1412**	-0.19765	-0.00235
ρ_b [g cm^{-3}]	0-20	NT-CC -- ST-CC	-0.0125	0.8472	-0.11015	0.085148
ρ_b [g cm^{-3}]	0-20	NT-CC -- ST-NO	0.0225	0.7292	-0.07515	0.120148
ρ_b [g cm^{-3}]	0-20	NT-NO -- ST-CC	0.0875	0.1933	-0.01015	0.185148
ρ_b [g cm^{-3}]	0-20	NT-NO -- ST-NO	0.1225	**0.0777**	0.024852	0.220148
ρ_b [g cm^{-3}]	0-20	ST-CC -- ST-NO	0.035	0.5916	-0.06265	0.132648
ρ_b [g cm^{-3}]	20-25	NT-CC -- NT-NO	-0.055	0.1984	-0.11714	0.007136
ρ_b [g cm^{-3}]	20-25	NT-CC -- ST-CC	0	1	-0.06214	0.062136
ρ_b [g cm^{-3}]	20-25	NT-CC -- ST-NO	-0.0325	0.4368	-0.09464	0.029636
ρ_b [g cm^{-3}]	20-25	NT-NO -- ST-CC	0.055	0.1984	-0.00714	0.117136
ρ_b [g cm^{-3}]	20-25	NT-NO -- ST-NO	0.0225	0.5878	-0.03964	0.084636
ρ_b [g cm^{-3}]	20-25	ST-CC -- ST-NO	-0.0325	0.4368	-0.09464	0.029636
θ_{-33kPa} [cm^3 cm^{-3}]	0-20	NT-CC -- NT-NO	-0.01017	0.5868	-0.03817	0.017834
θ_{-33kPa} [cm^3 cm^{-3}]	0-20	NT-CC -- ST-CC	-0.06136	**_0.0056_**	-0.08936	-0.03336
θ_{-33kPa} [cm^3 cm^{-3}]	0-20	NT-CC -- ST-NO	-0.03503	**0.0784**	-0.06303	-0.00703
θ_{-33kPa} [cm^3 cm^{-3}]	0-20	NT-NO -- ST-CC	-0.05119	**_0.0157_**	-0.07919	-0.02319
θ_{-33kPa} [cm^3 cm^{-3}]	0-20	NT-NO -- ST-NO	-0.02487	0.1971	-0.05287	0.003135
θ_{-33kPa} [cm^3 cm^{-3}]	0-20	ST-CC -- ST-NO	0.026326	0.1738	-0.00167	0.054328
θ_{-33kPa} [cm^3 cm^{-3}]	20-25	NT-CC -- NT-NO	-0.03819	**_0.0234_**	-0.06082	-0.01556
θ_{-33kPa} [cm^3 cm^{-3}]	20-25	NT-CC -- ST-CC	-0.05679	**_0.0023_**	-0.07942	-0.03417
θ_{-33kPa} [cm^3 cm^{-3}]	20-25	NT-CC -- ST-NO	-0.03436	**_0.0377_**	-0.05698	-0.01173
θ_{-33kPa} [cm^3 cm^{-3}]	20-25	NT-NO -- ST-CC	-0.0186	0.2301	-0.04123	0.004023
θ_{-33kPa} [cm^3 cm^{-3}]	20-25	NT-NO -- ST-NO	0.003836	0.7987	-0.01879	0.026462
θ_{-33kPa} [cm^3 cm^{-3}]	20-25	ST-CC -- ST-NO	0.022439	0.1531	-0.00019	0.045066
θ_{-10kPa} [cm^3 cm^{-3}]	0-20	NT-CC -- NT-NO	-0.01017	0.6712	-0.04613	0.025786
θ_{-10kPa} [cm^3 cm^{-3}]	0-20	NT-CC -- ST-CC	-0.04686	**0.0682**	-0.08282	-0.0109
θ_{-10kPa} [cm^3 cm^{-3}]	0-20	NT-CC -- ST-NO	-0.04269	**0.0929**	-0.07865	-0.00673
θ_{-10kPa} [cm^3 cm^{-3}]	0-20	NT-NO -- ST-CC	-0.03668	**0.1427**	-0.07264	-0.00072
θ_{-10kPa} [cm^3 cm^{-3}]	0-20	NT-NO -- ST-NO	-0.03251	0.1896	-0.06847	0.003448
θ_{-10kPa} [cm^3 cm^{-3}]	0-20	ST-CC -- ST-NO	0.00417	0.8614	-0.03179	0.04013
θ_{-10kPa} [cm^3 cm^{-3}]	20-25	NT-CC -- NT-NO	-0.0236	0.2088	-0.05092	0.003728
θ_{-10kPa} [cm^3 cm^{-3}]	20-25	NT-CC -- ST-CC	-0.04766	**_0.0199_**	-0.07498	-0.02033
θ_{-10kPa} [cm^3 cm^{-3}]	20-25	NT-CC -- ST-NO	-0.03037	**0.1131**	-0.05769	-0.00304
θ_{-10kPa} [cm^3 cm^{-3}]	20-25	NT-NO -- ST-CC	-0.02406	0.2006	-0.05139	0.003263
θ_{-10kPa} [cm^3 cm^{-3}]	20-25	NT-NO -- ST-NO	-0.00677	0.7099	-0.03409	0.020556
θ_{-10kPa} [cm^3 cm^{-3}]	20-25	ST-CC -- ST-NO	0.017293	0.3496	-0.01003	0.044618
Ks [log$_{10}$(cm d^{-1})]	0-20	NT-CC -- NT-NO	0.75351	**_0.0116_**	0.363698	1.143322
Ks [log$_{10}$(cm d^{-1})]	0-20	NT-CC -- ST-CC	0.337974	0.2071	-0.05184	0.727786
Ks [log$_{10}$(cm d^{-1})]	0-20	NT-CC -- ST-NO	0.570122	**_0.044_**	0.18031	0.959934
Ks [log$_{10}$(cm d^{-1})]	0-20	NT-NO -- ST-CC	-0.41554	**0.1271**	-0.80535	-0.02572
Ks [log$_{10}$(cm d^{-1})]	0-20	NT-NO -- ST-NO	-0.18339	0.4832	-0.5732	0.206424
Ks [log$_{10}$(cm d^{-1})]	0-20	ST-CC -- ST-NO	0.232148	0.3778	-0.15766	0.62196
Ks [log$_{10}$(cm d^{-1})]	20-25	NT-CC -- NT-NO	0.633404	**0.1155**	0.059248	1.20756

Variable [unit]	Depth Range [cm]	Comparison	Difference	P-value	LCL	UCL
Ks [log$_{10}$(cm d^{-1})]	20-25	NT-CC -- ST-CC	1.009435	**0.0192**	0.435279	1.583591
Ks [log$_{10}$(cm d^{-1})]	20-25	NT-CC -- ST-NO	0.900776	**0.0327**	0.32662	1.474932
Ks [log$_{10}$(cm d^{-1})]	20-25	NT-NO -- ST-CC	0.376031	0.3337	-0.19813	0.950187
Ks [log$_{10}$(cm d^{-1})]	20-25	NT-NO -- ST-NO	0.267372	0.4876	-0.30678	0.841528
Ks [log$_{10}$(cm d^{-1})]	20-25	ST-CC -- ST-NO	-0.10866	0.776	-0.68282	0.465497
PAW [cm^3 cm^{-3}]	0-20	NT-CC -- NT-NO	-0.02791	0.2175	-0.06088	0.005069
PAW [cm^3 cm^{-3}]	0-20	NT-CC -- ST-CC	-0.06189	**0.0137**	-0.09486	-0.02891
PAW [cm^3 cm^{-3}]	0-20	NT-CC -- ST-NO	-0.06563	**0.0099**	-0.0986	-0.03265
PAW [cm^3 cm^{-3}]	0-20	NT-NO -- ST-CC	-0.03398	**0.139**	-0.06696	-0.00101
PAW [cm^3 cm^{-3}]	0-20	NT-NO -- ST-NO	-0.03772	**0.104**	-0.0707	-0.00474
PAW [cm^3 cm^{-3}]	0-20	ST-CC -- ST-NO	-0.00374	0.8645	-0.03671	0.029238
PAW [cm^3 cm^{-3}]	20-25	NT-CC -- NT-NO	0.001511	0.9378	-0.02765	0.03067
PAW [cm^3 cm^{-3}]	20-25	NT-CC -- ST-CC	-0.03174	**0.12**	-0.0609	-0.00258
PAW [cm^3 cm^{-3}]	20-25	NT-CC -- ST-NO	-0.01075	0.5812	-0.03991	0.018411
PAW [cm^3 cm^{-3}]	20-25	NT-NO -- ST-CC	-0.03325	**0.1049**	-0.06241	-0.00409
PAW [cm^3 cm^{-3}]	20-25	NT-NO -- ST-NO	-0.01226	0.5301	-0.04142	0.0169
PAW [cm^3 cm^{-3}]	20-25	ST-CC -- ST-NO	0.020992	0.2899	-0.00817	0.050151
φ [cm^3 cm^{-3}]	0-20	NT-CC -- NT-NO	0.0375	0.1642	-0.00143	0.076427
φ [cm^3 cm^{-3}]	0-20	NT-CC -- ST-CC	0.005	0.8467	-0.03393	0.043927
φ [cm^3 cm^{-3}]	0-20	NT-CC -- ST-NO	-0.01	0.6997	-0.04893	0.028927
φ [cm^3 cm^{-3}]	0-20	NT-NO -- ST-CC	-0.0325	0.2234	-0.07143	0.006427
φ [cm^3 cm^{-3}]	0-20	NT-NO -- ST-NO	-0.0475	**0.0851**	-0.08643	-0.00857
φ [cm^3 cm^{-3}]	0-20	ST-CC -- ST-NO	-0.015	0.5644	-0.05393	0.023927
φ [cm^3 cm^{-3}]	20-25	NT-CC -- NT-NO	0.02	0.214	-0.00344	0.04344
φ [cm^3 cm^{-3}]	20-25	NT-CC -- ST-CC	-0.0025	0.8724	-0.02594	0.02094
φ [cm^3 cm^{-3}]	20-25	NT-CC -- ST-NO	0.01	0.5241	-0.01344	0.03344
φ [cm^3 cm^{-3}]	20-25	NT-NO -- ST-CC	-0.0225	0.1656	-0.04594	0.00094
φ [cm^3 cm^{-3}]	20-25	NT-NO -- ST-NO	-0.01	0.5241	-0.03344	0.01344
φ [cm^3 cm^{-3}]	20-25	ST-CC -- ST-NO	0.0125	0.4281	-0.01094	0.03594
θ$_{-1500kPa}$ [cm^3 cm^{-3}]	0-20	NT-CC -- NT-NO	0.01774	0.2361	-0.00414	0.039617
θ$_{-1500kPa}$ [cm^3 cm^{-3}]	0-20	NT-CC -- ST-CC	0.000529	0.9709	-0.02135	0.022406
θ$_{-1500kPa}$ [cm^3 cm^{-3}]	0-20	NT-CC -- ST-NO	0.030594	**0.0526**	0.008716	0.052471
θ$_{-1500kPa}$ [cm^3 cm^{-3}]	0-20	NT-NO -- ST-CC	-0.01721	0.2496	-0.03909	0.004666
θ$_{-1500kPa}$ [cm^3 cm^{-3}]	0-20	NT-NO -- ST-NO	0.012853	0.384	-0.00902	0.034731
θ$_{-1500kPa}$ [cm^3 cm^{-3}]	0-20	ST-CC -- ST-NO	0.030064	**0.0562**	0.008187	0.051942
θ$_{-1500kPa}$ [cm^3 cm^{-3}]	20-25	NT-CC -- NT-NO	-0.0397	**0.1168**	-0.07583	-0.00357
θ$_{-1500kPa}$ [cm^3 cm^{-3}]	20-25	NT-CC -- ST-CC	-0.02505	0.3072	-0.06119	0.011078
θ$_{-1500kPa}$ [cm^3 cm^{-3}]	20-25	NT-CC -- ST-NO	-0.02361	0.3348	-0.05974	0.012526
θ$_{-1500kPa}$ [cm^3 cm^{-3}]	20-25	NT-NO -- ST-CC	0.014648	0.5446	-0.02148	0.05078
θ$_{-1500kPa}$ [cm^3 cm^{-3}]	20-25	NT-NO -- ST-NO	0.016095	0.5063	-0.02004	0.052228
θ$_{-1500kPa}$ [cm^3 cm^{-3}]	20-25	ST-CC -- ST-NO	0.001447	0.9519	-0.03469	0.037579
θ$_{FC(3day)}$ [cm cm^{-1}]	0 – 20	NT-CC - NT-NO	0.015140174	0.3214	-0.00737	0.037654
θ$_{FC(3day)}$ [cm cm^{-1}]	0 – 20	NT-CC - ST-CC	7.06E-04	0.9623	-0.02181	0.02322
θ$_{FC(3day)}$ [cm cm^{-1}]	0 – 20	NT-CC - ST-NO	0.027982868	**0.0801**	0.005469	0.050497
θ$_{FC(3day)}$ [cm cm^{-1}]	0 - 20	NT-NO - ST-CC	-0.014434127	0.3436	-0.03695	0.00808
θ$_{FC(3day)}$ [cm cm^{-1}]	0 - 20	NT-NO - ST-NO	0.012842694	0.3976	-0.00967	0.035357
θ$_{FC(3day)}$ [cm cm^{-1}]	0 - 20	ST-CC - ST-NO	0.02727682	**0.0871**	0.004763	0.049791
θ$_{FC(3day)}$ [cm cm^{-1}]	20 - 40	NT-CC - NT-NO	-0.020299355	**0.0625**	-0.03551	-0.00509

Variable [unit]	Depth Range [cm]	Comparison	Difference	P-value	LCL	UCL
$\theta_{FC(3day)}$ [cm cm^{-1}]	20 - 40	NT-CC - ST-CC	-0.012484612	0.2307	-0.02769	0.002722
$\theta_{FC(3day)}$ [cm cm^{-1}]	20 - 40	NT-CC - ST-NO	-0.01359903	0.1942	-0.02881	0.001608
$\theta_{FC(3day)}$ [cm cm^{-1}]	20 - 40	NT-NO - ST-CC	0.007814743	0.4447	-0.00739	0.023022
$\theta_{FC(3day)}$ [cm cm^{-1}]	20 - 40	NT-NO - ST-NO	0.006700325	0.5109	-0.00851	0.021907
$\theta_{FC(3day)}$ [cm cm^{-1}]	20 - 40	ST-CC - ST-NO	-0.001114417	0.9121	-0.01632	0.014093
$\theta_{FC(3day)}$ [cm cm^{-1}]	40 - 60	NT-CC - NT-NO	-0.00296152	0.5114	-0.00969	0.003768
$\theta_{FC(3day)}$ [cm cm^{-1}]	40 - 60	NT-CC - ST-CC	-0.002087109	0.6419	-0.00882	0.004642
$\theta_{FC(3day)}$ [cm cm^{-1}]	40 - 60	NT-CC - ST-NO	-0.005187568	0.2587	-0.01192	0.001542
$\theta_{FC(3day)}$ [cm cm^{-1}]	40 - 60	NT-NO - ST-CC	8.74E-04	0.845	-0.00586	0.007604
$\theta_{FC(3day)}$ [cm cm^{-1}]	40 - 60	NT-NO - ST-NO	-0.002226048	0.6202	-0.00896	0.004503
$\theta_{FC(3day)}$ [cm cm^{-1}]	40 - 60	ST-CC - ST-NO	-0.003100459	0.4921	-0.00983	0.003629
$\theta_{FC(3day)}$ [cm cm^{-1}]	60 - 100	NT-CC - NT-NO	-0.002812337	0.4919	-0.00891	0.003289
$\theta_{FC(3day)}$ [cm cm^{-1}]	60 - 100	NT-CC - ST-CC	-0.001599995	0.6938	-0.0077	0.004501
$\theta_{FC(3day)}$ [cm cm^{-1}]	60 - 100	NT-CC - ST-NO	-0.004512793	0.2775	-0.01061	0.001589
$\theta_{FC(3day)}$ [cm cm^{-1}]	60 - 100	NT-NO - ST-CC	0.001212341	0.7652	-0.00489	0.007314
$\theta_{FC(3day)}$ [cm cm^{-1}]	60 - 100	NT-NO - ST-NO	-0.001700456	0.6758	-0.0078	0.004401
$\theta_{FC(3day)}$ [cm cm^{-1}]	60 - 100	ST-CC - ST-NO	-0.002912798	0.4769	-0.00901	0.003189
$\Delta W_{(3\,day)}$ [cm]	0 - 20	NT-CC - NT-NO	0.079245899	0.1537	-7.80E-04	0.159272
$\Delta W_{(3\,day)}$ [cm]	0 - 20	NT-CC - ST-CC	0.035343204	0.5099	-0.04468	0.115369
$\Delta W_{(3\,day)}$ [cm]	0 - 20	NT-CC - ST-NO	0.087166804	**0.1197**	0.007141	0.167193
$\Delta W_{(3\,day)}$ [cm]	0 - 20	NT-NO - ST-CC	-0.043902695	0.4153	-0.12393	0.036123
$\Delta W_{(3\,day)}$ [cm]	0 - 20	NT-NO - ST-NO	0.007920906	0.8815	-0.07211	0.087947
$\Delta W_{(3\,day)}$ [cm]	0 - 20	ST-CC - ST-NO	0.0518236	0.3389	-0.0282	0.13185
$\Delta W_{(3\,day)}$ [cm]	20 - 40	NT-CC - NT-NO	-0.051541149	**0.0353**	-0.08496	-0.01812
$\Delta W_{(3\,day)}$ [cm]	20 - 40	NT-CC - ST-CC	-0.020864525	0.3559	-0.05429	0.012557
$\Delta W_{(3\,day)}$ [cm]	20 - 40	NT-CC - ST-NO	-0.026390739	0.2479	-0.05981	0.007031
$\Delta W_{(3\,day)}$ [cm]	20 - 40	NT-NO - ST-CC	0.030676624	0.1835	-0.00274	0.064098
$\Delta W_{(3\,day)}$ [cm]	20 - 40	NT-NO - ST-NO	0.025150411	0.2696	-0.00827	0.058572
$\Delta W_{(3\,day)}$ [cm]	20 - 40	ST-CC - ST-NO	-0.005526213	0.8036	-0.03895	0.027895
$\Delta W_{(3\,day)}$ [cm]	40 - 60	NT-CC - NT-NO	-0.020754001	0.6743	-0.09487	0.053361
$\Delta W_{(3\,day)}$ [cm]	40 - 60	NT-CC - ST-CC	-0.016111982	0.7439	-0.09023	0.058003
$\Delta W_{(3\,day)}$ [cm]	40 - 60	NT-CC - ST-NO	-0.045683363	0.3618	-0.1198	0.028431
$\Delta W_{(3\,day)}$ [cm]	40 - 60	NT-NO - ST-CC	0.004642019	0.9249	-0.06947	0.078757
$\Delta W_{(3\,day)}$ [cm]	40 - 60	NT-NO - ST-NO	-0.024929362	0.6143	-0.09904	0.049185
$\Delta W_{(3\,day)}$ [cm]	40 - 60	ST-CC - ST-NO	-0.029571381	0.5509	-0.10369	0.044543
$\Delta W_{(3\,day)}$ [cm]	60 - 100	NT-CC - NT-NO	-0.054132329	0.5927	-0.20564	0.097372
$\Delta W_{(3\,day)}$ [cm]	60 - 100	NT-CC - ST-CC	-0.025543386	0.7998	-0.17705	0.125961
$\Delta W_{(3\,day)}$ [cm]	60 - 100	NT-CC - ST-NO	-0.088419413	0.3871	-0.23992	0.063085
$\Delta W_{(3\,day)}$ [cm]	60 - 100	NT-NO - ST-CC	0.028588943	0.7766	-0.12292	0.180094
$\Delta W_{(3\,day)}$ [cm]	60 - 100	NT-NO - ST-NO	-0.034287083	0.7338	-0.18579	0.117218
$\Delta W_{(3\,day)}$ [cm]	60 - 100	ST-CC - ST-NO	-0.062876027	0.5353	-0.21438	0.088629
Pores: <0.2 μm	0 - 5	NT-CC - NT-NO	0.002815389	**0**	0.002477	0.003153
Pores: <0.2 μm	0 - 5	NT-CC - ST-CC	0.002585408	**0**	0.002247	0.002924
Pores: <0.2 μm	0 - 5	NT-CC - ST-NO	0.002586301	**0**	0.002248	0.002924
Pores: <0.2 μm	0 - 5	NT-NO - ST-CC	-2.30E-04	0.4768	-5.68E-04	1.08E-04
Pores: <0.2 μm	0 - 5	NT-NO - ST-NO	-2.29E-04	0.4803	-5.67E-04	1.09E-04
Pores: <0.2 μm	0 - 5	ST-CC - ST-NO	8.93E-07	1	-3.37E-04	3.39E-04
Pores: 0.2-10 μm	0 - 5	NT-CC - NT-NO	-0.001562704	**0.0144**	-0.00266	-4.66E-04

Variable [unit]	Depth Range [cm]	Comparison	Difference	P-value	LCL	UCL
Pores: 0.2-10 µm	0 - 5	NT-CC - ST-CC	-6.15E-04	0.6364	-0.00171	4.82E-04
Pores: 0.2-10 µm	0 - 5	NT-CC - ST-NO	-0.00744646	**0**	-0.00854	-0.00635
Pores: 0.2-10 µm	0 - 5	NT-NO - ST-CC	9.47E-04	0.2625	-1.49E-04	0.002044
Pores: 0.2-10 µm	0 - 5	NT-NO - ST-NO	-0.005883755	**0**	-0.00698	-0.00479
Pores: 0.2-10 µm	0 - 5	ST-CC - ST-NO	-0.006831157	**0**	-0.00793	-0.00573
Pores: 10-50 µm	0 - 5	NT-CC - NT-NO	-0.002561805	**0**	-0.00305	-0.00207
Pores: 10-50 µm	0 - 5	NT-CC - ST-CC	-0.00292541	**0**	-0.00342	-0.00243
Pores: 10-50 µm	0 - 5	NT-CC - ST-NO	-0.003151266	**0**	-0.00364	-0.00266
Pores: 10-50 µm	0 - 5	NT-NO - ST-CC	-3.64E-04	0.4018	-8.56E-04	1.29E-04
Pores: 10-50 µm	0 - 5	NT-NO - ST-NO	-5.89E-04	**0.0572**	-0.00108	-9.66E-05
Pores: 10-50 µm	0 - 5	ST-CC - ST-NO	-2.26E-04	0.7663	-7.19E-04	2.67E-04
Pores: 50-1000 µm	0 - 5	NT-CC - NT-NO	0.001801894	**0**	0.00127	0.002334
Pores: 50-1000 µm	0 - 5	NT-CC - ST-CC	0.001597245	**0**	0.001065	0.002129
Pores: 50-1000 µm	0 - 5	NT-CC - ST-NO	0.003943534	**0**	0.003411	0.004476
Pores: 50-1000 µm	0 - 5	NT-NO - ST-CC	-2.05E-04	0.8483	-7.37E-04	3.27E-04
Pores: 50-1000 µm	0 - 5	NT-NO - ST-NO	0.00214164	**0**	0.00161	0.002674
Pores: 50-1000 µm	0 - 5	ST-CC - ST-NO	0.002346288	**0**	0.001814	0.002878
Pores: <0.2 µm	20 - 25	NT-CC - NT-NO	3.40E-04	**0**	2.94E-04	3.87E-04
Pores: <0.2 µm	20 - 25	NT-CC - ST-CC	8.57E-04	**0**	8.10E-04	9.03E-04
Pores: <0.2 µm	20 - 25	NT-CC - ST-NO	8.68E-04	**0**	8.22E-04	9.15E-04
Pores: <0.2 µm	20 - 25	NT-NO - ST-CC	5.16E-04	**0**	4.70E-04	5.63E-04
Pores: <0.2 µm	20 - 25	NT-NO - ST-NO	5.28E-04	**0**	4.81E-04	5.74E-04
Pores: <0.2 µm	20 - 25	ST-CC - ST-NO	1.14E-05	0.9543	-3.50E-05	5.79E-05
Pores: 0.2-10 µm	20 - 25	NT-CC - NT-NO	0.008308039	**0**	0.007172	0.009444
Pores: 0.2-10 µm	20 - 25	NT-CC - ST-CC	0.003161296	**0**	0.002025	0.004298
Pores: 0.2-10 µm	20 - 25	NT-CC - ST-NO	0.00445459	**0**	0.003318	0.005591
Pores: 0.2-10 µm	20 - 25	NT-NO - ST-CC	-0.005146743	**0**	-0.00628	-0.00401
Pores: 0.2-10 µm	20 - 25	NT-NO - ST-NO	-0.003853449	**0**	-0.00499	-0.00272
Pores: 0.2-10 µm	20 - 25	ST-CC - ST-NO	0.001293294	**0.0772**	1.57E-04	0.00243
Pores: 10-50 µm	20 - 25	NT-CC - NT-NO	-1.08E-04	0.9915	-8.98E-04	6.82E-04
Pores: 10-50 µm	20 - 25	NT-CC - ST-CC	-8.86E-04	**0.0841**	-0.00168	-9.65E-05
Pores: 10-50 µm	20 - 25	NT-CC - ST-NO	-2.75E-04	0.8822	-0.00106	5.15E-04
Pores: 10-50 µm	20 - 25	NT-NO - ST-CC	-7.78E-04	0.1601	-0.00157	1.17E-05
Pores: 10-50 µm	20 - 25	NT-NO - ST-NO	-1.67E-04	0.9702	-9.57E-04	6.23E-04
Pores: 10-50 µm	20 - 25	ST-CC - ST-NO	6.12E-04	0.3581	-1.78E-04	0.001401
Pores: 50-1000 µm	20 - 25	NT-CC - NT-NO	-0.004292887	**0**	-0.00494	-0.00365
Pores: 50-1000 µm	20 - 25	NT-CC - ST-CC	-0.001873353	**0**	-0.00252	-0.00123
Pores: 50-1000 µm	20 - 25	NT-CC - ST-NO	-0.001031633	**0.0043**	-0.00168	-3.87E-04
Pores: 50-1000 µm	20 - 25	NT-NO - ST-CC	0.002419534	**0**	0.001775	0.003064
Pores: 50-1000 µm	20 - 25	NT-NO - ST-NO	0.003261254	**0**	0.002617	0.003906
Pores: 50-1000 µm	20 - 25	ST-CC - ST-NO	8.42E-04	**0.0304**	1.97E-04	0.001486

Data availability

660 The data and processing code used in this study are available at https://github.com/saraya209/Araya_etal_2021_SOIL_Data_and_Code [*will be deposited at Zonedo.org and a doi created upon acceptance of the manuscript for publication*].

Author contribution

All co-authors contributed to the study design. Sampling was carried out by SA and TA. Soil analysis and modeling were 665 carried out by SA with supervision from TA. SA prepared the manuscript with contributions from all co-authors.

Acknowledgments

This work was made possible with support from the Conservation Agriculture Systems Project and the California Department of Water Resources.

Deleted: soil

Deleted: for

Deleted: *deposited*

Deleted: *on Figshare.com*

References

Abdalla, M., Hastings, A., Cheng, K., Yue, Q., Chadwick, D., Espenberg, M., Truu, J., Rees, R. M., and Smith, P.: A critical review of the impacts of cover crops on nitrogen leaching, net greenhouse gas balance and crop productivity, Glob. Chang. Biol., 25, 2530–2543, https://doi.org/10.1111/gcb.14644, 2019.

Abdollahi, L., Schjønning, P., Elmholt, S., and Munkholm, L. J.: The effects of organic matter application and intensive tillage and traffic on soil structure formation and stability, Soil Tillage Res., 136, 28–37, https://doi.org/10.1016/j.still.2013.09.011, 2014.

Allen, R. G., Pereira, L. S., Raes, D., and Smith, M.: Crop evapotranspiration: Guidelines for computing crop water requirements - FAO Irrigation and drainage paper 56, Food and Agriculture Organization of the United Nations, Rome, Italy, 1998.

Alletto, L., Pot, V., Giuliano, S., Costes, M., Perdrieux, F., and Justes, E.: Temporal variation in soil physical properties improves the water dynamics modeling in a conventionally-tilled soil, Geoderma, 243–244, 18–28, https://doi.org/10.1016/j.geoderma.2014.12.006, 2015.

Alvarez, R. and Steinbach, H. S.: A review of the effects of tillage systems on some soil physical properties, water content, nitrate availability and crops yield in the Argentine Pampas, Soil Tillage Res., 104, 1–15, https://doi.org/10.1016/J.STILL.2009.02.005, 2009.

Angers, D. A. and Caron, J.: Plant-induced Changes in Soil Structure: Processes and Feedbacks, Biogeochemistry, 42, 55–72, https://doi.org/10.1023/A:1005944025343, 1998.

Ashworth, A. J., DeBruyn, J. M., Allen, F. L., Radosevich, M., and Owens, P. R.: Microbial community structure is affected by cropping sequences and poultry litter under long-term no-tillage, Soil Biol. Biochem., 114, 210–219, https://doi.org/10.1016/J.SOILBIO.2017.07.019, 2017.

Assouline, S. and Or, D.: The concept of field capacity revisited: Defining intrinsic static and dynamic criteria for soil internal drainage dynamics, Water Resour. Res., 50, 4787–4802, https://doi.org/10.1002/2014WR015475, 2014.

Bacq-Labreuil, A., Crawford, J., Mooney, S. J., Neal, A. L., and Ritz, K.: Cover crop species have contrasting influence upon soil structural genesis and microbial community phenotype, Sci. Rep., 9, 7473, https://doi.org/10.1038/s41598-019-43937-6, 2019.

Baker, J. B., Southard, R. J., and Mitchell, J. P.: Agricultural Dust Production in Standard and Conservation Tillage Systems in the San Joaquin Valley, J. Environ. Qual., 34, 1260, https://doi.org/10.2134/jeq2003.0348, 2005.

Basche, A. and DeLonge, M.: The Impact of Continuous Living Cover on Soil Hydrologic Properties: A Meta-Analysis, Soil Sci. Soc. Am. J., 81, 1179, https://doi.org/10.2136/sssaj2017.03.0077, 2017.

Basche, A. D., Archontoulis, S. V., Kaspar, T. C., Jaynes, D. B., Parkin, T. B., and Miguez, F. E.: Simulating long-term impacts of cover crops and climate change on crop production and environmental outcomes in the Midwestern United States, Agric. Ecosyst. Environ., 218, 95–106, https://doi.org/10.1016/J.AGEE.2015.11.011, 2016a.

Basche, A. D., Kaspar, T. C., Archontoulis, S. V., Jaynes, D. B., Sauer, T. J., Parkin, T. B., and Miguez, F. E.: Soil water improvements with the long-term use of a winter rye cover crop, Agric. Water Manag., 172, 40–50, https://doi.org/10.1016/j.agwat.2016.04.006, 2016b.

710 Bilek, M.: Winter annual rye cover crops in no-till grain crop rotations: impacts on soil physical properties and organic matter, University of Maryland, College Park, 2007.

Blanco-Canqui, H. and Ruis, S. J.: No-tillage and soil physical environment, Geoderma, 326, 164–200, https://doi.org/10.1016/j.geoderma.2018.03.011, 2018.

Büchi, L., Wendling, M., Amossé, C., Necpalova, M., and Charles, R.: Importance of cover crops in alleviating negative effects
715 of reduced soil tillage and promoting soil fertility in a winter wheat cropping system, Agric. Ecosyst. Environ., 256, 92–104, https://doi.org/10.1016/j.agee.2018.01.005, 2018.

Burr-Hersey, J. E., Mooney, S. J., Bengough, A. G., Mairhofer, S., and Ritz, K.: Developmental morphology of cover crop species exhibit contrasting behaviour to changes in soil bulk density, revealed by X-ray computed tomography, PLoS One, 12, e0181872, https://doi.org/10.1371/journal.pone.0181872, 2017.

720 Duchene, O., Vian, J.-F., and Celette, F.: Intercropping with legume for agroecological cropping systems: Complementarity and facilitation processes and the importance of soil microorganisms. A review, Agric. Ecosyst. Environ., 240, 148–161, https://doi.org/10.1016/J.AGEE.2017.02.019, 2017.

Durner, W.: Hydraulic conductivity estimation for soils with heterogeneous pore structure, Water Resour. Res., 30, 211–223, https://doi.org/10.1029/93WR02676, 1994.

725 Ekschmitt, K., Kandeler, E., Poll, C., Brune, A., Buscot, F., Friedrich, M., Gleixner, G., Hartmann, A., Kästner, M., Marhan, S., Miltner, A., Scheu, S., and Wolters, V.: Soil-carbon preservation through habitat constraints and biological limitations on decomposer activity, J. Plant Nutr. Soil Sci., 171, 27–35, https://doi.org/10.1002/jpln.200700051, 2008.

Faunt, C. C.: Alluvial Boundary of California's Central Valley [Map]. Scale Not Given, https://water.usgs.gov/lookup/getspatial?pp1766_Alluvial_Bnd, 2012.

730 Fernandez, A. L., Sheaffer, C. C., Wyse, D. L., Staley, C., Gould, T. J., and Sadowsky, M. J.: Structure of bacterial communities in soil following cover crop and organic fertilizer incorporation, Appl. Microbiol. Biotechnol., 100, 9331–9341, https://doi.org/10.1007/s00253-016-7736-9, 2016.

Finney, D. M., Buyer, J. S., and Kaye, J. P.: Living cover crops have immediate impacts on soil microbial community structure and function, J. Soil Water Conserv., 72, 361–373, https://doi.org/10.2489/jswc.72.4.361, 2017.

735 Gao, L., Becker, E., Liang, G., Houssou, A. A., Wu, H., Wu, X., Cai, D., and Degré, A.: Effect of different tillage systems on aggregate structure and inner distribution of organic carbon, Geoderma, 288, 97–104, https://doi.org/10.1016/j.geoderma.2016.11.005, 2017.

Gao, L., Wang, B., Li, S., Wu, H., Wu, X., Liang, G., Gong, D., Zhang, X., Cai, D., and Degré, A.: Soil wet aggregate distribution and pore size distribution under different tillage systems after 16 years in the Loess Plateau of China, 173, 38–47,
740 https://doi.org/10.1016/j.catena.2018.09.043, 2019.

van Genuchten, M. T.: A Closed-form Equation for Predicting the Hydraulic Conductivity of Unsaturated Soils, https://doi.org/10.2136/sssaj1980.03615995004400050002x, 1980.

González-Sánchez, E. J., Kassam, A., Basch, G., Streit, B., Holgado-Cabrera, A., and Triviño-Tarradas, P.: Conservation Agriculture and its contribution to the achievement of agri-environmental and economic challenges in Europe, AIMS Agric. Food, https://doi.org/10.3934/agrfood.2016.4.387, 2016.

Green, T. R., Ahuja, L. R., and Benjamin, J. G.: Advances and challenges in predicting agricultural management effects on soil hydraulic properties, Geoderma, 116, 3–27, https://doi.org/10.1016/S0016-7061(03)00091-0, 2003.

Greenland, D. J.: Soil Damage by Intensive Arable Cultivation: Temporary or Permanent?, Philos. Trans. R. Soc. B Biol. Sci., 281, 193–208, https://doi.org/10.1098/rstb.1977.0133, 1977.

Grossman, R. B. and Reinsch, T. G.: Bulk Density and Linear Extensibility, in: Methods of Soil Analysis, Part 4--Physical Methods, edited by: Dane, J. H. and Topp, G. C., Soil Science Society of America, Madison, Wisconsin, 201–228, https://doi.org/10.2136/sssabookser5.4.c9, 2002.

Hillel, D.: Environmental Soil Physics, Academic Press, San Diego, CA, 1998.

Hudson, B. D.: Soil organic matter and available water capacity, J. Soil Water Conserv., 49, 189–194, 1994.

Janzen, H. H.: Beyond carbon sequestration: soil as conduit of solar energy, Eur. J. Soil Sci., 66, 19–32, https://doi.org/10.1111/ejss.12194, 2015.

Janzen, H. H., Janzen, D. W., and Gregorich, E. G.: The 'soil health' metaphor: illuminating or illusory?, Soil Biol. Biochem., 108167, https://doi.org/10.1016/j.soilbio.2021.108167, 2021.

Jarvis, N. J.: A review of non-equilibrium water flow and solute transport in soil macropores: principles, controlling factors and consequences for water quality, Eur. J. Soil Sci., 58, 523–546, https://doi.org/10.1111/j.1365-2389.2007.00915.x, 2007.

Johnson, A. M. M. and Hoyt, G. D. D.: Changes to the soil environment under conservation tillage, Horttechnology, 9, 380–393, https://doi.org/10.21273/HORTTECH.9.3.380, 1999.

Kassam, A., Friedrich, T., and Derpsch, R.: Global spread of Conservation Agriculture, Int. J. Environ. Stud., 76, 29–51, https://doi.org/10.1080/00207233.2018.1494927, 2019.

Kastanek, F. J. and Nielsen, D. R.: Description of Soil Water Characteristics Using Cubic Spline Interpolation, Soil Sci. Soc. Am. J., 65, 279, https://doi.org/10.2136/sssaj2001.652279x, 2001.

Klute, A.: Water Retention: Laboratory Methods, in: Methods of Soil Analysis: Part 1, Physical and Mineralogical Methods, 5.1, edited by: Klute, A., Madison, Wisconsin, USA, 635–662, https://doi.org/10.2136/sssabookser5.1.2ed.c26, 1986.

Lal, R., Reicosky, D. C., and Hanson, J. D.: Evolution of the plow over 10,000 years and the rationale for no-till farming, Soil Tillage Res., 93, 1–12, https://doi.org/10.1016/j.still.2006.11.004, 2007.

Lehmann, J. and Kleber, M.: The contentious nature of soil organic matter, Nature, 528, 60–68,

https://doi.org/10.1038/nature16069, 2015.

Li, Y., Chang, S. X., Tian, L., and Zhang, Q.: Conservation agriculture practices increase soil microbial biomass carbon and nitrogen in agricultural soils: A global meta-analysis, Soil Biol. Biochem., 121, 50–58, https://doi.org/10.1016/j.soilbio.2018.02.024, 2018.

Liu, J., Macrae, M. L., Elliott, J. A., Baulch, H. M., Wilson, H. F., and Kleinman, P. J. A.: Impacts of Cover Crops and Crop Residues on Phosphorus Losses in Cold Climates: A Review, J. Environ. Qual., 0, 0, https://doi.org/10.2134/jeq2019.03.0119, 2019.

Madden, N. M., Southard, R. J., and Mitchell, J. P.: Conservation tillage reduces PM10 emissions in dairy forage rotations, Atmos. Environ., 42, 3795–3808, https://doi.org/10.1016/j.atmosenv.2007.12.058, 2008.

Mapa, R. B., Green, R. E., and Santo, L.: Temporal Variability of Soil Hydraulic Properties with Wetting and Drying Subsequent to Tillage, Soil Sci. Soc. Am. J., 50, 1133, https://doi.org/10.2136/sssaj1986.03615995005000050008x, 1986.

Martens, D. A.: Nitrogen cycling under different soil management systems, 143–192, https://doi.org/10.1016/s0065-2113(01)70005-3, 2004.

Meurer, K., Barron, J., Chenu, C., Coucheney, E., Fielding, M., Hallett, P., Herrmann, A. M., Keller, T., Koestel, J., Larsbo, M., Lewan, E., Or, D., Parsons, D., Parvin, N., Taylor, A., Vereecken, H., and Jarvis, N.: A framework for modelling soil structure dynamics induced by biological activity, Glob. Chang. Biol., 26, 5382–5403, https://doi.org/10.1111/gcb.15289, 2020.

Mitchell, J. P.: Conservation agriculture: systems thinking for sustainable farming, Calif. Agric., 70, 53–55, 2016.

Mitchell, J. P., Klonsky, K. M., Miyao, E. M., and Hembree, K. J.: Conservation tillage tomato production in California's San Joaquin Valley, Agric. Nat. Resour., 2009.

Mitchell, J. P., Klonsky, K. M., Miyao, E. M., Aegerter, B. J., Shrestha, A., Munk, D. S., Hembree, K. J., Madden, N. M., and Turini, T. A.: Evolution of Conservation Tillage Systems for Processing Tomato in California's Central Valley, Horttechnology, 22, 617–626, 2012.

Mitchell, J. P., Shrestha, A., Horwath, W. R., Southard, R. J., Madden, N. M., Veenstra, J. J., and Munk, D. S.: Tillage and Cover Cropping Affect Crop Yields and Soil Carbon in the San Joaquin Valley, California, Agron. J., 107, 588, https://doi.org/10.2134/agronj14.0415, 2015.

Mitchell, J. P., Carter, L. M., Reicosky, D. C., Shrestha, A., Pettygrove, G. S., Klonsky, K. M., Marcum, D. B., Chessman, D., Roy, R., Hogan, P., and Dunning, L.: A history of tillage in California's Central Valley, Soil Tillage Res., 157, 52–64, https://doi.org/10.1016/j.still.2015.10.015, 2016a.

Mitchell, J. P., Shrestha, A., and Munk, D. S.: Cotton response to long-term no-tillage and cover cropping in the San Joaquin Valley, J. Cotton Sci., 20, 8–17, 2016b.

Mitchell, J. P., Shrestha, A., Dahlberg, J. A., Munk, D. S., and Hembree, K. J.: Prospect of No-till Planting of Sorghum with and without Cover Cropping in the San Joaquin Valley, Crop. Forage Turfgrass Manag., 2, 0,

805   https://doi.org/10.2134/cftm2015.0208, 2016c.

Mitchell, J. P., Shrestha, A., Mathesius, K., Scow, K. M., Southard, R. J., Haney, R. L., Schmidt, R., Munk, D. S., and Horwath, W. R.: Cover cropping and no-tillage improve soil health in an arid irrigated cropping system in California's San Joaquin Valley, USA, Soil Tillage Res., 165, 325–335, https://doi.org/10.1016/j.still.2016.09.001, 2017.

Mitchell, J. P., Reicosky, D. C., Kueneman, E. A., Fisher, J., and Beck, D.: Conservation agriculture systems, CAB Rev.
810   Perspect. Agric. Vet. Sci. Nutr. Nat. Resour., 14, https://doi.org/10.1079/PAVSNNR201914001, 2019.

Moret, D. and Arrúe, J. L.: Dynamics of soil hydraulic properties during fallow as affected by tillage, Soil Tillage Res., 96, 103–113, https://doi.org/10.1016/j.still.2007.04.003, 2007.

Naab, J. B., Mahama, G. Y., Yahaya, I., and Prasad, P. V. V: Conservation Agriculture Improves Soil Quality, Crop Yield, and Incomes of Smallholder Farmers in North Western Ghana., Front. Plant Sci., 8, 996,
815   https://doi.org/10.3389/fpls.2017.00996, 2017.

National Cooperative Soil Survey: National Cooperative Soil Survey Characterization Database, http://ncsslabdatamart.sc.egov.usda.gov/.

Or, D., Leij, F. J., Snyder, V., and Ghezzehei, T. A.: Stochastic model for posttillage soil pore space evolution, Water Resour. Res., 36, 1641–1652, https://doi.org/10.1029/2000WR900092, 2000.

820   Palm, C., Blanco-Canqui, H., DeClerck, F., Gatere, L., and Grace, P.: Conservation agriculture and ecosystem services: An overview, Agric. Ecosyst. Environ., 187, 87–105, https://doi.org/10.1016/J.AGEE.2013.10.010, 2014.

Peña-Sancho, C., López, M. V., Gracia, R., and Moret-Fernández, D.: Effects of tillage on the soil water retention curve during a fallow period of a semiarid dryland, Soil Res., 55, 114, https://doi.org/10.1071/SR15305, 2016.

Pires, L. F., Cássaro, F. A. M., Reichardt, K., and Bacchi, O. O. S.: Soil porous system changes quantified by analyzing soil
825   water retention curve modifications, Soil Tillage Res., 100, 72–77, https://doi.org/10.1016/j.still.2008.04.007, 2008.

Pires, L. F., Borges, J. A. R., Rosa, J. A., Cooper, M., Heck, R. J., Passoni, S., and Roque, W. L.: Soil structure changes induced by tillage systems, Soil Tillage Res., 165, 66–79, https://doi.org/10.1016/j.still.2016.07.010, 2017.

Pittelkow, C. M., Linquist, B. A., Lundy, M. E., Liang, X., van Groenigen, K. J., Lee, J., van Gestel, N., Six, J., Venterea, R. T., and van Kessel, C.: When does no-till yield more? A global meta-analysis, F. Crop. Res., 183, 156–168,
830   https://doi.org/10.1016/J.FCR.2015.07.020, 2015.

R Core Team: R: A Language and Environment for Statistical Computing, https://www.r-project.org/, 2019.

Rasmussen, K. J.: Impact of ploughless soil tillage on yield and soil quality: A Scandinavian review, Soil Tillage Res., 53, 3–14, https://doi.org/10.1016/S0167-1987(99)00072-0, 1999.

Rath, D., Bogie, N., Deiss, L., Parikh, S., Wang, D., Ying, S., Tautges, N., Berhe, A. A., and Scow, K.: Synergy between
835   compost and cover crops leads to increased subsurface soil carbon storage, SOIL Discuss., 1–27, https://doi.org/10.5194/soil-2021-19, 2021.

Reicosky, D. C. and Allmaras, R. R.: Advances in Tillage Research in North American Cropping Systems, J. Crop Prod., 8, 75–125, https://doi.org/10.1300/J144v08n01_05, 2003.

Reicosky, D. C. and Forcella, F.: Cover crop and soil quality interactions in agroecosystems, J. Soil Water Conserv., 53, 224–229, 1998.

Sanz-Cobena, A., Lassaletta, L., Aguilera, E., Prado, A. del, Garnier, J., Billen, G., Iglesias, A., Sánchez, B., Guardia, G., Abalos, D., Plaza-Bonilla, D., Puigdueta-Bartolomé, I., Moral, R., Galán, E., Arriaga, H., Merino, P., Infante-Amate, J., Meijide, A., Pardo, G., Álvaro-Fuentes, J., Gilsanz, C., Báez, D., Doltra, J., González-Ubierna, S., Cayuela, M. L., Menéndez, S., Díaz-Pinés, E., Le-Noë, J., Quemada, M., Estellés, F., Calvet, S., van Grinsven, H. J. M., Westhoek, H., Sanz, M. J., Gimeno, B. S., Vallejo, A., and Smith, P.: Strategies for greenhouse gas emissions mitigation in Mediterranean agriculture: A review, Agric. Ecosyst. Environ., 238, 5–24, https://doi.org/10.1016/J.AGEE.2016.09.038, 2017.

Sastre, B., Marques, M. J., García-Díaz, A., and Bienes, R.: Three years of management with cover crops protecting sloping olive groves soils, carbon and water effects on gypsiferous soil, 171, 115–124, https://doi.org/10.1016/j.catena.2018.07.003, 2018.

Schaap, M. G., Leij, F. J., and van Genuchten, M. T.: Rosetta: A computer program for estimating soil hydraulic parameters with hierarchical pedotransfer functions, J. Hydrol., 251, 163–176, https://doi.org/10.1016/S0022-1694(01)00466-8, 2001.

Schmidt, M. W. I., Torn, M. S., Abiven, S., Dittmar, T., Guggenberger, G., Janssens, I. A., Kleber, M., Kogel-Knabner, I., Lehmann, J., Manning, D. A. C., Nannipieri, P., Rasse, D. P., Weiner, S., and Trumbore, S. E.: Persistence of soil organic matter as an ecosystem property, Nature, 478, 49–56, https://doi.org/Doi 10.1038/Nature10386, 2011.

Schwen, A., Bodner, G., Scholl, P., Buchan, G. D., and Loiskandl, W.: Temporal dynamics of soil hydraulic properties and the water-conducting porosity under different tillage, Soil Tillage Res., 113, 89–98, https://doi.org/10.1016/j.still.2011.02.005, 2011.

Shelton, D., Jasa, P., Brown, L., and Hirschi, M.: Water Erosion, in: Conservation Tillage Systems and Management, edited by: Ames, I., MidWest Plan Service, Iowa State University. MWPS-45, 2000.

Simunek, J., van Genuchten, M. T., and Sejna, M.: The HYDRUS Software Package for Simulating Two- and Three-Dimensional Movement of Water, Heat, and Multiple Solutes in Variably-Saturated Porous Media, Technical Manual, Version 2.0, https://www.pc-progress.com/downloads/Pgm_Hydrus3D2/HYDRUS3D Technical Manual.pdf, 2012.

Strudley, M., Green, T., and Ascough II, J.: Tillage effects on soil hydraulic properties in space and time: State of the science, Soil Tillage Res., 99, 4–48, https://doi.org/10.1016/j.still.2008.01.007, 2008.

Tautges, N. E., Chiartas, J. L., Gaudin, A. C. M., O'Geen, A. T., Herrera, I., and Scow, K. M.: Deep soil inventories reveal that impacts of cover crops and compost on soil carbon sequestration differ in surface and subsurface soils, Glob. Chang. Biol., 25, 3753–3766, https://doi.org/10.1111/gcb.14762, 2019.

Tavares Filho, J. and Tessier, D.: Characterization of soil structure and porosity under long-term conventional tillage and no-tillage systems, Rev. Bras. Ciência do Solo, 33, 1837–1844, https://doi.org/10.1590/S0100-06832009000600032, 2009.

Twarakavi, N. K. C., Sakai, M., and Simunek, J.: An objective analysis of the dynamic nature of field capacity, Water Resour.

Res., 45, 1–9, https://doi.org/10.1029/2009WR007944, 2009.

Upadhyaya, S. K., Lancas, K. P., Santos-Filho, A. G., and Raghuwanshi, N. S.: One-pass tillage equipment outstrips conventional tillage method, Calif. Agric., 55, 44–47, https://doi.org/10.3733/ca.v055n05p44, 2001.

Veenstra, J. J., Horwath, W. R., Mitchell, J. P., and Munk, D. S.: Conservation tillage and cover cropping influence soil properties in SanJoaquin Valley cotton-tomato crop, Calif. Agric., 60, 146–153, 2006.

Veenstra, J. J., Horwath, W. R., and Mitchell, J. P.: Tillage and Cover Cropping Effects on Aggregate-Protected Carbon in Cotton and Tomato, Soil Sci. Soc. Am. J., 71, 362, https://doi.org/10.2136/sssaj2006.0229, 2007.

Veihmeyer, F. J. and Hendrickson, A. H.: The moisture equivalent as a measure of the field capacity of soils, SOIL Sci., 32, 181–193, https://doi.org/10.1097/00010694-193109000-00003, 1931.

Veloso, M. G., Angers, D. A., Tiecher, T., Giacomini, S., Dieckow, J., and Bayer, C.: High carbon storage in a previously degraded subtropical soil under no-tillage with legume cover crops, Agric. Ecosyst. Environ., 268, 15–23, https://doi.org/10.1016/j.agee.2018.08.024, 2018.

Vereecken, H., Schnepf, A., Hopmans, J. W., Javaux, M., Or, D., Roose, T., Vanderborght, J., Young, M. H., Amelung, W., Aitkenhead, M., Allison, S. D., Assouline, S., Baveye, P., Berli, M., Bruggemann, N., Finke, P., Flury, M., Gaiser, T., Govers, G., Ghezzehei, T., Hallett, P., Hendricks Franssen, H. J., Heppell, J., Horn, R., Huisman, J. A., Jacques, D., Jonard, F., Kollet, S., Lafolie, F., Lamorski, K., Leitner, D., McBratney, A., Minasny, B., Montzka, C., Nowak, W., Pachepsky, Y. A., Padarian, J., Romano, N., Roth, K., Rothfuss, Y., Rowe, E. C., Schwen, A., Simunek, J., Tiktak, A., Van Dam, J., van der Zee, S. E. A. T. M., Vogel, H. J., Vrugt, J. A., Wohling, T., and Young, I. M.: Modeling Soil Processes: Review, Key Challenges, and New Perspectives, Vadose Zo. J., 15, 0, https://doi.org/10.2136/vzj2015.09.0131, 2016.

Villamil, M. B., Bollero, G. A., Darmody, R. G., Simmons, F. W., and Bullock, D. G.: No-Till Corn/Soybean Systems Including Winter Cover Crops, Soil Sci. Soc. Am. J., 70, 1936, https://doi.org/10.2136/sssaj2005.0350, 2006.

Vrugt, J. A., van Wijk, M. T., Hopmans, J. W., and Šimunek, J.: One-, two-, and three-dimensional root water uptake functions for transient modeling, Water Resour. Res., 37, 2457–2470, https://doi.org/10.1029/2000WR000027, 2001.

Zuber, S. M. and Villamil, M. B.: Meta-analysis approach to assess effect of tillage on microbial biomass and enzyme activities, Soil Biol. Biochem., 97, 176–187, https://doi.org/10.1016/j.soilbio.2016.03.011, 2016.